

Zero-Shot Action Recognition in Videos: A Survey

Valter Estevam^{a,c,*}, Helio Pedrini^b, David Menotti^c

^a*Federal Institute of Paraná, Irati-PR, 84500-000, Brazil*

^b*University of Campinas, Institute of Computing, Campinas-SP, 13083-852, Brazil*

^c*Federal University of Paraná, Department of Informatics, Curitiba-PR, 81531-970, Brazil*

Abstract

Zero-Shot Action Recognition has attracted attention in the last years and many approaches have been proposed for recognition of objects, events and actions in images and videos. There is a demand for methods that can classify instances from classes that are not present in the training of models, especially in the complex problem of automatic video understanding, since collecting, annotating and labeling videos are difficult and laborious tasks. We have identified that there are many methods available in the literature, however, it is difficult to categorize which techniques can be considered state of the art. Despite the existence of some surveys about zero-shot action recognition in still images and experimental protocol, there is no work focused on videos. Therefore, we present a survey of the methods that comprise techniques to perform visual feature extraction and semantic feature extraction as well to learn the mapping between these features considering specifically zero-shot action recognition in videos. We also provide a complete description of datasets, experiments and protocols, presenting open issues and directions for future work, essential for the development of the computer vision research field.

Keywords: Zero-shot learning, Video action recognition, Visual embedding, Semantic label embedding, Experimental protocols, Deep features

1. Introduction

In recent years, many works in the computer vision field have explored the human action or activity recognition problem using still images or videos. Some authors, such as Turaga et al. [93], define actions as simple motion patterns often performed by only one human being, and activities as more complex patterns that involve coordinated actions of a small group of humans. However, there is no universal understanding of these concepts in the literature. In this text, we adopt the term action recognition to refer to both concepts, regardless of whether the authors consider their work as action or activity recognition. Following this assumption, several surveys [93, 71, 2, 28, 117, 44] show approaches addressing the Human Action Recognition (HAR) problem by proposing new visual or semantic features describing the actions more accurately. For example, the Dense Trajectory Features (DTF) [97] and its variant, the Improved Dense Trajectories (IDT) [96],

are two successful methods based on handcrafted visual features. Another group of works explores semantic features, such as poses and poselets [1], objects [32], scenes [114] and attributes [115], or investigates new inference methods, such as in [57]. Recently, deep learning has been applied to HAR, leveraging visual features through the exploration of convolution operation, temporal modeling, and multi-stream configuration, as shown by Kong and Fu [44].

All these approaches suffer from inherent drawbacks, for example: (i) they do not generalize very well on large and complex datasets, such as Charades [84] or Kinetics [12]; (ii) the handcraft visual features are very expensive to compute; (iii) manual-annotated semantic features require heavy human labor or expert knowledge, which are not always available; and (iv) many labeled examples are required to reduce the generalization problem when deep learning is used.

In a real-world scenario, there are many more actions than in the academic benchmark datasets used to learn the models. Moreover, the new examples may be unlabeled, which makes the supervised methods inappropriate. In this context, Zero-Shot Learning (ZSL) emerges

*Corresponding author

Email address: valter.junior@ifpr.edu.br (Valter Estevam)

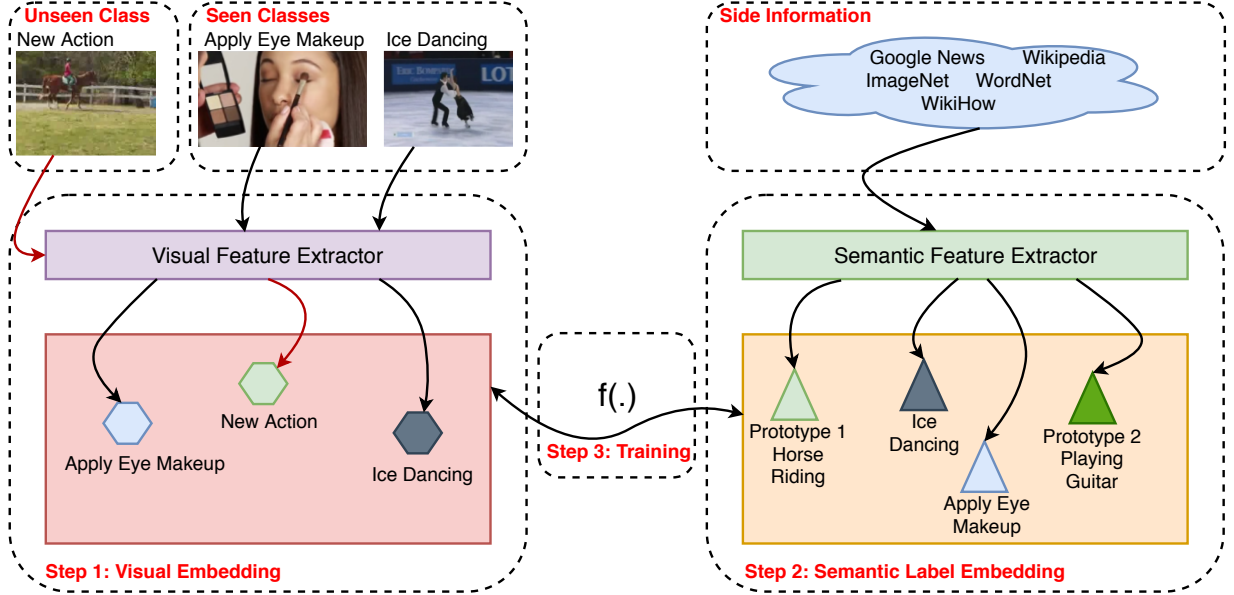


Figure (1) Schematic representation of a ZSL human action recognition framework.

attempting to overcome these limitations.

The human ability to recognize an action without ever having seen it before, that is, associating semantic information from several sources to the visual appearance of actions, is the inspiration of ZSL approaches [43]. In Figure 1, we provide an overview of ZSL approaches considering the application in videos. This general scheme can also be found in ZSL applied to object and event recognition in both images and videos [22]. We introduce the main aspects of the approaches throughout this text.

In this example, some videos from Apply Eye Makeup and Ice Dancing action classes are used to extract visual features in order to compose a visual space. Commonly, these visual features are obtained using the IDT method [97], Histogram of Gradient (HoG), Histogram of Optical Flow (HoF), and Motion Boundary Histogram (MBH) algorithms with Bag-of-Features approach [78]; or using deep features from Convolutional 3D Network (C3D) [90] or Inflated 3D Network (I3D) [12].

In ZSL, we assume that we have a set of all possible action class labels, and, for some of them, there is no video example. Therefore, auxiliary semantic side information is required to provide a computational representation for the labels. This representation usually relies on attributes manually annotated [75], word vectors [43] and hierarchical structures [4], which are called prototypes. If we try to recognize a new video from the New Action class, which has never been seen

before, in addition to extracting visual features, it is necessary to associate them with a suitable prototype and assign a label. This is made by learning an $f(\cdot)$ mapping function between these spaces. As discussed in Section 3, this mapping function can assume several ways to be performed directly into the semantic space, indirectly by creating an intermediate space or directly into the visual space.

Thus, we concentrate our investigation in approaches that address the problem of recognizing human actions, without having seen them before, in small video clips, typically with less than 10 seconds. This is referred to as Zero-Shot Action Recognition (ZSAR) problem¹. We do not take into account the Few-Shot Learning (FSL) task since it is a different problem. In FSL, the presence of some examples usually introduces a significant disturbance in the probability distribution of the representations, which degrades the performance over both class groups (i.e., with many and few examples). Works focused on FSL usually perform a matching between a query video and the representative videos of each class, and the general problem is how to create better representations in order to allow this matching. Some examples are shown in [7, 26, 116].

There exist other surveys related to ZSL. For instance, Fu et al. [22] and Xian et al. [105] provided

¹Throughout this text, when the term ZSAR is used, it refers to ZSAR in videos, rather than ZSAR in images. The latter is not widely studied and its approaches are more similar to ZSL applied to object recognition than the ZSAR techniques covered by this text.

an overview of ZSL problems, especially about still images and experimental protocols. More recently, Wang et al. [102] investigated the ZSL paradigm with focus on settings, methods and applications for actions, objects and events. Although some initial works in ZSAR adopted approaches inspired by zero-shot object recognition, covered by other surveys, there are several approaches specially designed for ZSAR that deserve attention. To the best of our knowledge, there is no survey focused on ZSAR in videos and our main contributions are three-fold: (i) to provide a complete description of ZSL methods applied to human action recognition in videos detailing the methods used to extract visual features, semantic features, as well to perform the training; (ii) to present a discussion about the limitations of the benchmark datasets and evaluation protocols adopted in works in the literature; and (iii) to identify open issues pointing future research strategies, based on the natural evolution of the ZSAR approaches, and inspire different approaches in this knowledge domain.

The remainder of the text is organized as follows. We review the methods used to perform visual and semantic embedding in Section 2 and provide a complete description of ZSAR approaches in Section 3. The benchmark datasets are presented in Section 4, whereas experimental protocols and performance are discussed in Section 5. We discuss open issues and directions for future work in Section 6. Finally, some concluding remarks are presented in Section 7.

2. Visual and Semantic Label Embedding Steps

Two crucial steps in any ZSAR method are the visual and semantic label embeddings. They are responsible for providing the features used to map the visual appearance to the semantic description of actions.

2.1. Visual Embedding Step

In the visual embedding step, some methods, in most cases off-the-shelf, are used to process the visual information. These methods explore contiguous or sampled sequences of frames extracting global or local representations or identifying humans and objects and also how they interact with each other or evolve in the video clips. Figure 2 illustrates a video segment processed with different methods.

We catalogue a set of methods used to perform visual embedding in the investigated literature, as shown in Table 1. Next, we also provide a brief review of these methods.

Bag-of-Features (BoF) methods are used in [78, 75, 54, 79, 21]. In the first ZSL work in videos [54], the

visual words were obtained from a descriptor composed of spatio-temporal volumes and 1D Gabor detector. In later works, a well known combination of HoG, HoF, and MBH descriptors was used.

However, more promising results were achieved with an improved BoF descriptor, DTF, proposed in [94] and used in [106, 27]. The DTF is able to characterize shape (point coordinates), appearance (Histogram of Gradient), motion (Histogram of Optical Flow) and variations on motion (Motion Boundary Histogram). The *dense* term refers to initial sampling in each frame with a grid of $W \times W$ points combined with spatio-temporal pyramid approach, as shown in Figure 2 (a) (on the left).

Table (1) Methods used to perform visual embedding in ZSAR Handcrafted Features (HF) and Deep Features (DF).

Method		Used in approaches
HF	BoF	Liu et al. [54], Qiu et al. [75], Fu et al. [21], Rohrbach et al. [78], Rohrbach et al. [79]
		DTF
	IDT	Xu et al. [106], Guadarrama et al. [27]
		Kodirov et al. [43], Gan et al. [24], Xu et al. [108], Xu et al. [107], Xu et al. [109], Gan et al. [23], Alexiou et al. [5], Fu et al. [19], Zhang and Peng [113], Liu et al. [56], Wang and Chen [99]
DF	From [46]	Jain et al. [34]
	VGG	Gan et al. [23], Zhang and Peng [113], Wu et al. [103]
	ResNet-50	Bishay et al. [7]
	ResNet-200	Zhu et al. [116]
	3D CNN	Mishra et al. [65]
	C3D	Wang and Chen [100], Liu et al. [56], Zhang et al. [112], Hahn et al. [29], Wang and Chen [98], Bishay et al. [7], Mandal et al. [59], Mishra et al. [64], Brattoli et al. [10]
	I3D	Roitberg et al. [80], Ghosh et al. [26], Mandal et al. [59], Piergiovanni and Ryoo [70]
	R(2+1)D	Brattoli et al. [10]
	Other	Li et al. [52]

Since it is not possible to apply tracking in homogeneous regions of video frames, these points are removed from sampling. For each remaining point in each frame, the dense flow field is computed, and subsequent frames are concatenated to create a trajectory descriptor. Next, static trajectories of each sampled point are also removed (Figure 2 (a) (center)). Then, descriptors are computed from spatio-temporal volumes with $N \times N \times L$

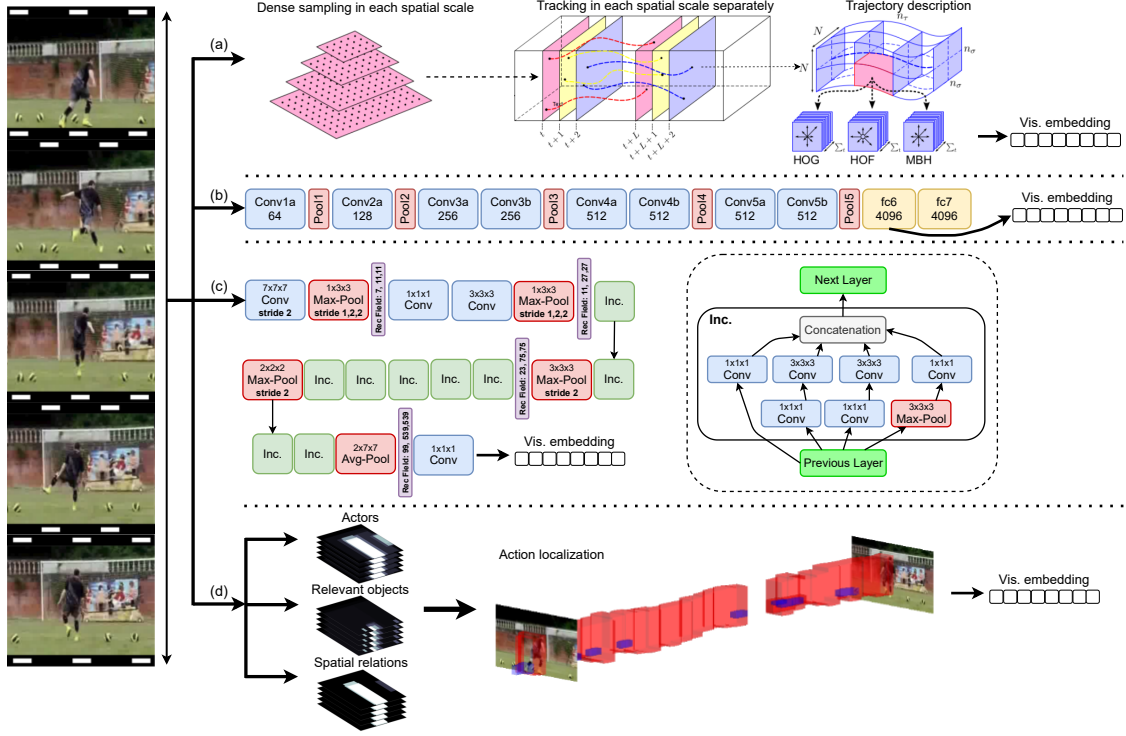


Figure (2) Some visual embedding strategies that receive a common video clip and generate an array that represents global handcrafted features (a), deep features with temporal modeling ((b) and (c)), and actor-object relationships over the scene (d). The methods are (a) Dense trajectories [94], (b) C3D [90], (c) I3D [12] and (d) Spatial-Aware Object Embeddings [61].

dimension (e.g., $5 \text{ pixels} \times 5 \text{ pixels} \times 15 \text{ frames}$), subdivided in $n_\sigma \times n_\sigma \times n_\tau$ cells (e.g., $2 \times 2 \times 3$), as shown in Figure 2 (a) (on the right). In the end, a codebook for each descriptor (trajectory, HoG, HoF, MBH) is created by fixing the number of visual words per descriptor to 4000 and performing k -means algorithm eight times, while keeping the results with the lowest error. The resulting histograms of visual words are used as a global video representation.

As shown in [95], the performance of the HoF descriptor degrades significantly in the presence of camera motion (e.g., pan, tilt and zoom). Hence, the IDT method [97] provides a mechanism to cancel out the camera motion from optical flow in the tracking phase, and a human detector [73] is used to remove trajectories in regions where humans are not found. This method presents a promising performance and is used in many works (see Table 1). However, it is computationally intensive and becomes impracticable on large-scale datasets [90, 56].

Deep learning has attracted much attention in recent years due to its advances in several problems such as: image classification [72], hand gesture recognition [45], licence plate recognition [50], and spoofing

detection [60]). In these applications, it is common to employ deep models pre-trained in large-scale datasets, and this ability is the major motivation for their use in ZSAR. For example, a Convolutional Neural Network (CNN) pre-trained on the ImageNet dataset [14], called VGG 19 [85], is used in [23], providing a detector for 1000 different concepts from individual frames. In their work, videos are represented in terms of detected visual concepts that are classified as relevant or irrelevant according to their similarity with a given textual query. Jain et al. [34] also proposed an approach that relates objects and actions using the ImageNet dataset for training a CNN model from [46]. In [116], a ResNet-200 model is initially trained on ImageNet and fine-tuned on ActivityNet dataset [30]. However, such image-based deep models are not suitable for direct video representation due to the lack of motion modeling, as demonstrated in [90]. This problem can be overcome with deep models that consider spatio-temporal relations, providing features from their fully connected layers (fc). This strategy is applied in [65] using 3D Convolutional Neural Network (3D CNN) [35], in [100, 112, 56, 29, 98] using C3D [90], and in [80, 70] using I3D [12].

In the C3D network [90], full video frames are taken

as input and do not require any preprocessing except to resize frames to 128×171 pixels. To propagate spatio-temporal information across all the layers, 3D convolutional filters (3×3×3 with stride 1×1×1) and 3D pooling layers (2×2×2 with stride 2×2×2) are used. The architecture has two fully connected layers and a softmax output layer, which is removed to extract the visual embedding representation, as shown in Figure 2 (b). This model is trained on Sports-1M Dataset [40] and the visual representation is extracted from fc6 layer resulting in a vector with 4096 dimensions which are usually used without modifications or fine-tuning. An exception occurs in [112], in which the dimensionality is reduced to 500 using Principal Component Analysis (PCA).

Training 3D CNN consists of learning many more parameters than 2D CNN. Therefore, the I3D architecture [12] (Figure 2 (c)) uses a common pre-trained ImageNet Inception-V1 model [33] as base network, adding a batch normalization to each convolution layer. To properly explore spatio-temporal ordering and long-range dependencies, it uses a Long Short-Term Memory (LSTM) layer after the last average pooling layer of the Inception-V1. Additionally, its performance can be improved by including an optical-flow stream [12]. This model is shown in Figure 2 (c). The I3D model is trained on Kinetics dataset [12], and the visual representation is extracted from the last fully connected layer resulting in a representation of 256 dimensions in [80] and 1024 in [70]. It is likely that ZSL assumption (classes disjunction between the training and testing sets) has been violated since both C3D and I3D models are pre-trained on large-scale datasets [56]. Thus, a new problem emerges through the use of deep learning techniques. We present a detailed discussion on this topic in Section 5. Although simple and relatively effective, recent works have shown significantly gain in performance when these off-the-shelf global descriptors are fine-tuned, used to model temporal or spatial relationships, or conditioned by semantic information to produce new representations.

2.2. Semantic Label Embedding Step

Providing meaningful semantic information in ZSAR is a challenging task. On one hand, we can utilize attribute-based approaches, that have several drawbacks, such as: (i) annotating videos is more difficult than annotating images; (ii) in a more complex or complete dataset, several attributes are necessary to alleviate the semantic intraclass variability; (iii) it is difficult to define what attributes are relevant, and (iv) this approach is not scalable. On the other hand, we can utilize textual corpus information, which typically relies

on exploring unsupervised word embedding methods, gaining with a scalable process but losing performance. Figure 3 illustrates some strategies to perform semantic embedding. Next, we detail the main approaches.

Table (2) Methods used to perform semantic embedding in ZSAR. Attribute (A) and Word Embedding (WE).

	Method	Used in approaches
A	Annotated	Wang and Chen [99], Fu et al. [19], Mishra et al. [65], Liu et al. [54], Rohrbach et al. [78], Gan et al. [24], Fu et al. [21], Bishay et al. [7], Mandal et al. [59], Mishra et al. [64]
	Dictionary learning	Qiu et al. [75], Kodirov et al. [43]
	Dynamic	Jones et al. [38]
WE	Semantic hierarchies	Rohrbach et al. [79], Gan et al. [24]
	Knowledge graphs	Ghosh et al. [26], Gao et al. [25]
	Word2Vec	Xu et al. [106], Xu et al. [108], Xu et al. [107], Jain et al. [34], Gan et al. [23], Alexiou et al. [5], Li et al. [52], Wu et al. [103], Xu et al. [109], Wang and Chen [100], Qin et al. [74], Mishra et al. [65], Wang and Chen [99], Liu et al. [56], Brattoli et al. [10], Zhu et al. [116], Roitberg et al. [80], Mandal et al. [59], Bishay et al. [7], Roitberg et al. [81], Hahn et al. [29], Mishra et al. [64], Mettes and Snoek [61]
	GloVe	Zhang et al. [112], Piergiovanni and Ryoo [70], Zhang and Peng [113], Guadarrama et al. [27]

As shown in Table 2, using manually defined and annotated attributes is a common strategy [99, 65, 19, 54, 78, 24, 21]. An expert needs to define all attributes and also their values. These annotations can be made directly (e.g., annotations from UCF101, or USAA (Figure 3a)); or acquired by processing textual descriptions in the form of script-data (Figure 3c, collected with Amazon Mechanical Turk (AMT), as described by Rohrbach et al. [79]. Alternatively, dictionary learning techniques are proposed in [75, 43]. In these works, visual features are related to atoms in the automatically learned dictionary, alleviating the problem of manual definition of attributes.

Recently, methods based on word embedding have become popular (Table 2). For example, semantic hierarchies are mined for subjects, verbs, and objects using the descriptions of videos from YouTube [27] (Figure 3d) and WordNet [17] hierarchy was used

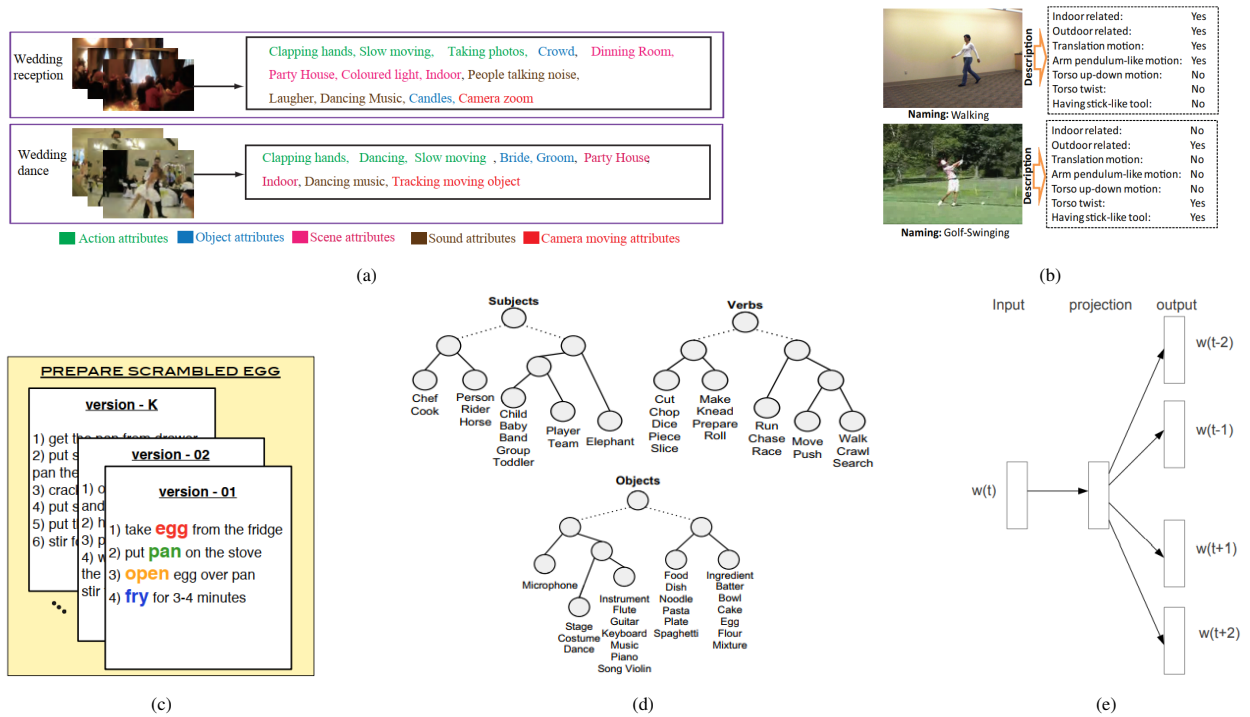


Figure (3) Main strategies for performing semantic label embedding in ZSAR. (a) The methods proposed by Fu et al. [20] and (b) Liu et al. [54] are attribute-based. (c) The approach developed by Rohrbach et al. [79] is a script-data representation. (d) The scheme proposed by Guadarrama et al. [27] is a semantic hierarchy; (e) The approach developed by Mikolov et al. [62] is an unsupervised word embedding method.

by Rohrbach et al. [79] to represent the action labels. However, the most popular strategy for semantic label embedding is the skip-gram model [63] (Figure 3e), more specifically the Word2Vec implementation [62] used in a wide variety of works (see Table 2). This model is an efficient method for learning vector representations that captures a large number of syntactic and semantic word relationships [62]. The method consists of learning a neural network that calculates a similarity measure between words based on a softmax output. In ZSL, the semantic vector representation for the interest word (action label) is based on the activation of 300 neurons in a hidden layer of the skip-gram network when this word is provided as input.

Another approach to performing semantic label embedding is a count-based model called Global Vectors (GloVe) [68]. In that model, a large matrix of co-occurrence statistics is constructed by storing words in rows and contexts in columns. Semantic vectors are learned such that their dot product equals the co-occurrence probability [3]. Intuitively, these statistics encode the meaning of words since the frequency of semantically similar words is higher than semantically dissimilar words. This word embedding property can be observed in Figure 4 with the class pairs Playing

Cello-Playing Piano, Apply Eye Makeup-Apply Lipstick in both Figures 4a and 4b. In these figures, 10 class representations from UCF101, acquired with Word2Vec and GloVe, were projected onto 2-dimensional spaces using the t-sne method [58]. We adopt a general approach to combine two or more word embeddings with a simple average of them. This approach is efficient but, in some cases, produces semantic imprecision as in the cases of Horse Race-Horse Riding, distant from each other in 4a, or Pommel Horse-Horse Race close to each other. Therefore, strategies based on textual descriptions or action-object relationships are successful and expected in future works.

3. Zero-Shot Action Recognition Approaches

The central problem in ZSAR is how to use visual and semantic information to classify new instances from unseen classes (i.e., to perform transfer knowledge). We identify three main approaches: (i) to classify directly into the semantic embedding space, usually projecting the visual features on it; (ii) to classify into an intermediate space generated with some combination technique for both visual and semantic representation (e.g.,

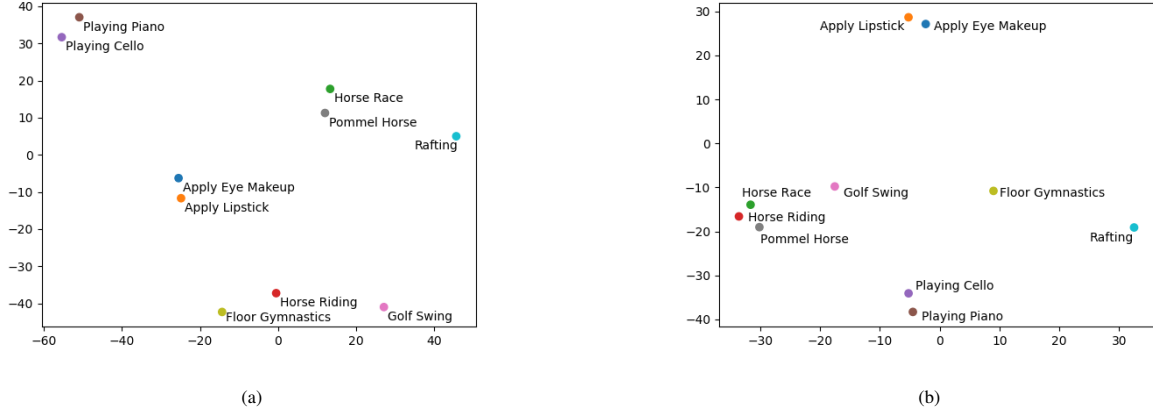


Figure (4) Word embeddings of 10 classes from UCF101 using in (a) Word2Vec [62] and (b) GloVe [68] methods. In both cases, the original representations have their dimensionality reduced using t-sne [58].

latent attributes or co-occurrence of actions and objects) and; (iii) to classify into the visual embedding space by synthesizing visual features conditioned by semantic side information in order to produce visual prototypes for unseen classes. Many other taxonomies could be proposed. However, ZSAR methods combine multiple strategies, so that provide unambiguous classifications is very difficult. Table 3 presents the methods and their classification according to our general criteria, and we also provide some observations.

In the next subsections, we explain the general ideas of these methods with a common notation and avoiding math complications whenever possible. In ZSAR, there are two datasets: the first is the training dataset $D_{tr} = \{(x_n, y_n)\}_{n=1}^{N_s}$, and the second is the testing dataset $D_{te} = \{(x_n, y_n)\}_{n=1}^{N_u}$, where x_n and y_n are, respectively, the visual representation and the class label for the n -th video sample v_n , N_s is the number of seen examples, and N_u is the number of unseen examples. The label spaces are $\mathcal{S} = \{1, 2, \dots, S\}$ and $\mathcal{U} = \{S+1, S+2, \dots, U\}$ with $\mathcal{S} \cap \mathcal{U} = \emptyset$. The visual feature is embedded with a function $E_v(v_n) = x_n$ so that $x_n \in R^d$. As discussed earlier, the function E_v may be represented by the methods DTF, IDT or C3D, for example, as illustrated in Figure 2. Similarly, the semantic embedding function for each class label is $E_l(y_n) = z_n$ so that $z_n \in R^m$. The E_l function usually corresponds to manual attribute annotation, data-driven attributes, learned hierarchies or word vectors, as shown in Figure 3.

3.1. Classification into the semantic embedding space

Many works try to learn a function $p : \mathbf{x} \rightarrow \mathbf{z}$ to project a visual representation x_n onto the semantic space obtaining a z'_n representation. Then, a function

$q : \mathbf{z}' \rightarrow \mathbf{y}$ is learned. In most cases this q function is a simple nearest neighbor classifier. However, Liu et al. [54] proposed a latent Support Vector Machine (SVM) formulation for the p function. In this case, m individual attribute classifiers (p_m) maps each representation x to the i -th correspondent attribute of z (i.e., each dimension). They do not use only annotated attributes, but also learn data-driven attributes by clustering low-level features maximizing the system information gain and using these features as latent variables. An unseen instance is classified using the p_m functions to project the raw visual features onto the semantic space and performing a nearest neighbour classification with Euclidean distance.

Fu et al. [20] introduced an attribute learning method based on the Probabilistic Topic Model (PTM) with Latent Dirichlet Allocation (LDA) [9]. In [21], they present the Multi-Modal Latent Attribute Topic Model (M2LATM) that extends that prior method. The new formulation considers three types of attributes: user-defined (UD), from any prior ontology (e.g., USAA dataset), latent class-conditional (CC), discriminative for known classes, and generalized free (GF), which represents shared aspects not presented in the attribute ontology. The major difference to [20] is the adaptation of PTM to work unconstrained. For example, UD topics are constrained in 1 to 1 correspondence with attributes from the ontology, and latent CC topics are constrained to match the class label. On the other hand, GF attributes are unconstrained. In both works, the classification occurs using a nearest neighbor rule using cosine distance. Another similar work appears in [75]. In this case, the p function corresponds to a dictionary learning method via information maximization. Both

Table (3) Overview of zero-shot human action recognition methods in videos. We organize the methods into three categories: classification into the semantic space, classification into an intermediate space, and classification into the visual space. For each approach, we point out the main strategies adopted.

Classification into the semantic space	
Reference	Main strategies
Liu et al. [54]	Single task learning with support vector machine
Fu et al. [20]	PTM + LDA + NN
Fu et al. [21]	PTM + LDA + NN + unconstrained attribute learning
Qiu et al. [75]	Sparse dictionary learning
Rohrbach et al. [79]	Text score + NN or SVM
Rohrbach et al. [78]	Text score + NN or SVM + transductive setting
Xu et al. [106]	Non-linear SVR with kernel RBF_{χ^2}
Xu et al. [109]	Manifold RR + transd. setting + data augmentation
Kodirov et al. [43]	Dictionary learning + regularised sparse coding
Li et al. [52]	MLP + convex combination of similar embedding
Hahn et al. [29]	Temporal modeling with LSTM + verb relationships
Alexiou et al. [5]	Semantic improvements with synonyms + self training
Bishay et al. [7]	Relation networks with segment-by-segment attention
Brattoli et al. [10]	End-to-end model with linear classifier + cross-dataset
Classification into an intermediate space	
Reference	Main strategies
Xu et al. [107]	Multi-task learning + prioritized data augmentation
Fu et al. [19]	Multi-view embedding space + CCA
Wang and Chen [99]	Landmark-based learning + sammon mapping + ST + SP
Wang and Chen [98]	Exploring texts and images for semantic embedding
Wang and Chen [100]	Multi-label ZSL + new split scheme
Gan et al. [24]	Concept detectors using least square regression (LR)
Zhu et al. [116]	Universal representation with GMIL + NMF
Mishra et al. [65]	Linear combinations of basis vectors (Gaussian params)
Mishra et al. [64]	Synthesized features with IAF and bi-di GAN
Qin et al. [74]	Visual embedding with error correcting output codes
Guadarrama et al. [27]	Semantic hierarchies for subjects, objects and verbs
Jain et al. [34]	Affinity between objects and classes
Wu et al. [103]	Semantic fusion network for objects, scenes and actions
Poppe [71]	Spatial-aware object embedding in action tubes
Gao et al. [25]	Action-object relationship modeled with GCN
Zhang et al. [112]	Multi-modal learning using video and text pairing
Piergiovanni and Ryoo [70]	Video and text encoding with unpaired data
Jones et al. [38]	Dynamic attributes signatures + finite state machines
Ghosh et al. [26]	Knowledge graphs learning + GCN
Classification into the visual space	
Reference	Main strategies
Zhang and Peng [113]	Joint distribution of visual and semantic knowledge
Mandal et al. [59]	Synthesized features + out-of-distribution classifier

appearance information between dictionary atoms and class label information are combined in order to learn a compact and discriminative dictionary for human action attributes.

Some approaches use only predefined semantic attributes. For example, Rohrbach et al. [78] proposed to associate scores of visual features with semantic attributes based on visual-annotation alignment, contextual, and co-occurrence information of the attributes. In their work, basic-level cooking actions such as fry or open and their related objects, egg or pan, are taken as attributes. Side information from cooking scripts (i.e., script-data shown in Figure 3c) is used to select the most relevant attributes based on statistical scores (frequency and term frequency \times inverse document frequency) as in [79]. The association between weighted attributes with the action label is learned using a nearest neighbor or a SVM classifier. They investigated a transductive setting by constructing a k-nearest neighbor (k -NN) graph calculating weights for instances in the semantic attribute space instead of the visual space. This approach exploits the manifold structure by utilizing the attributes from unknown classes without their class labels. The raw visual features (e.g., DTF) are used to learn m classifiers for each attribute, in a similar manner to [49]. Then, the probability of new classes is estimated with script-data.

Manual attributes have inherent limitations early discussed. Therefore, motivated by the success of the word vectors in language processing, many works try to extend their approaches to use this type of representation. Xu et al. [106] proposed an approach to project the low-level visual features obtained with MBH and HoG onto a semantic space of 300-dimensions composed by word vectors from Word2Vec [63]. They trained a non-linear Support Vector Regression (SVR) with RBF- χ^2 kernel defined as

$$K(x_i, x_j) = \exp(-\gamma \cdot D(x_i, x_j)), \quad (1)$$

where $D(x_i, x_j)$ is the χ^2 distance between histogram-based representations x_i and x_j to project new instances and classify with the nearest neighbour rule. Approaches similar to this formulation suffer severely with the domain shift problem because the probability distribution of seen classes is different from unseen ones. In their work, this problem is tackled with a transductive self-training procedure, and a data augmentation is conducted.

Subsequently, in [108], the authors proposed improvements in that approach using a manifold-regularized regression (semi-supervised learning). As

observed by Dinu et al. [16], in higher dimensional spaces, some instances from different classes may appear closest to each other, which is called the hubness problem. To tackle this problem and leverage the accuracy, they adapted the manifold-regularized regression to explore the manifold structure of unseen classes in a transductive setting.

Simple projection methods do not treat suitably the differences between class distributions of seen and unseen datasets. Hence, they are prone to suffer from the domain shift problem. To alleviate this problem, Kodirov et al. [43] proposed an unsupervised domain adaptation model by regularized sparse coding. In their work, each dimension of the semantic embedding space corresponds to a dictionary basis vector z_i with m dimensions. If the visual features are represented by a vector \mathbf{x}_i with d dimensions, a dictionary $D^{d \times m}$ can be learned using quadratic optimization so that the reconstruction error of $\mathbf{x}_i = D\mathbf{z}_i$ is minimized. Two dictionaries are learned, one to the source dataset D_s and another to the target dataset D_t . The domain shift is tackled by adding two constraints: D_t should be similar to D_s and, a visual-semantic similarity constraint given by the closeness of the interpretations of target data z'_i to their true class prototype z_i . Once trained, D_t is used to project the raw example onto the semantic space, and the nearest neighbor classifier assigns a label. Another strategy is to apply a label propagation across multiple semantic spaces, which are combined with a graph similarity matrix.

Li et al. [52] proposed to learn a common embedding space using a Multi-Layer Perceptron (MLP) to project visual features onto a 300-dimensional space where the class prototypes from Word2Vec are. The visual feature comes from a composition of two CNN outputs. The first for appearance patterns (i.e., RGB flow) and the second for motion patterns (i.e., Optical Flow). The last fully connected layers of these models are combined and used as input to the MLP. A new strategy to domain adaptation called Convex Combination of Similar Semantic Embedding Vectors (ConSSEV) is proposed. The main idea is to adjust the semantic output from MLP by creating a new vector weighted by the sum of all k highest similar vectors. This similarity is given by the MLP softmax outputs.

A similar strategy is presented in [29], but including temporal modeling. In their work, the videos are represented in a scheme in which the visual features are slightly related to corresponding verbs represented as word embeddings from Word2Vec method. In this method, until 21 short clips per video are fed to a C3D model obtaining 21 vectors with 4096 dimensions. Af-

ter, these vectors are grouped into 7 groups of 3 vectors each and used to train a network composed by 2-layer LSTM units and a fully-connected layer with 300 dimensions. The network is trained with a loss function defined as a sum of a cross-entropy loss (L_{CE}) and a pairwise-ranking loss (L_{PR}) defined as

$$L_{PR} = \min_{\theta} \sum_i \sum_x (1 - s(a_i, v_i)) + \max\{0, s(a_x, v_i)\} + \max\{0, s(a_i, v_x)\}, \quad (2)$$

where s is a similarity function (e.g., cosine similarity), v_i is a verb embedding of a class i (i.e., their word vector), a_i is the embedding of action-video, a_x is an action-video embedding of contrastive class k , and v_x is a contrastive verb embedding of class k . Zero-shot classification is performed by inputting a new example into the neural network and looking by the nearest neighbor of their 300-dimensional representation of the verbs into the semantic space.

Alexiou et al. [5] explored the impact of using class label synonyms on enhancing word vector representations. They mine a list of synonyms from multiple dictionaries for each class word vectors. These synonyms update the class word vector representations by weighting them based on the distances of actions and their synonyms. They also explored a self-training strategy, and the results using ZSAR methods based on direct projection point out to accuracy improvements. However, the comparisons with other methods are difficult due to experimental protocol differences.

Bishay et al. [7] proposed a method for FSL that can be adapted to ZSL. Their main idea for FSL is to estimate a deep similarity score among a query video and representative videos from each class assigning the label correspondent to the maximum score. In ZSL, this similarity is estimated among a query video and semantic embedding vectors representing the class labels. The model architecture in ZSL configuration has two modules: embedding and relation. The embedding module has two elements, the first one for visual embedding compound by a C3D network pre-trained on Sports-1M and the second one to semantic embedding compound by a skip-gram model. The relation module implements a segment-by-segment-attention mechanism that estimates the similarity between the semantic vector and each query video segment. The comparison outputs are aggregated over all segments using fully connected layers and an average pooling layer producing a final relation score. In the experiments, they adopt 50%/50% and 80%/20% random splits with 30 trials. They did not inform if overlapping classes between their test set

and the training set used in the pre-training deep model (C3D) were removed. Therefore, the results can violate the ZSL restriction.

More recently, Brattoli et al. [10] proposed the first end-to-end approach in ZSAR. In their method, both visual embedding and semantic embedding are learned and optimized at a same time. The visual embedding is acquired using $R(2 + 1)D$ [92] or C3D [90] architectures. The output of these models is $B \times T \times 512$, where B is the batch size and T the number of clips (1 in training and 1 or more in testing). E_s is a linear classifier with 512×300 weights, and, therefore, the output of $E_s \circ E_v$ is of shape $B \times 300$. A Word2Vec is incorporated given representations for all labels with 300-d. The loss function adopted consists of minimizing Equation 3.

$$L = \sum \| W2V(c) - (E_s \circ E_v)(x') \|^2 \quad (3)$$

Their work adopts a more realistic scenario cross dataset, where no overlapping between seen and pre-training classes are required to preserve the ZSL restriction. The similarity evaluation between class labels follows the protocol proposed by Roitberg et al. [81], where a label must be conveniently distant from any class label used to train the model.

3.2. Classification into an intermediate space

The techniques surveyed in this subsection create an intermediate space by projecting both visual embedding E_v and the semantic embedding E_s onto a new common t -dimensional space q , where $q \in R^t$. Typically, the visual projection occurs such as in the direct projection approaches, such that is necessary to develop methods suitable to project the semantic features onto this new subspace, which is the main focus of these approaches.

Xu et al. [107] proposed a Multi-Task Learning (MTL) approach instead of learning m classifiers (e.g., single task ridge regression [108]). They argue that single-task leads to overfitting because they assume each dimension independently, disregarding their relationships. With MTL, the parameters of all tasks lie on a low dimensional manifold. They also proposed a prioritized auxiliary data augmentation² for domain adaptation by selecting the most relevant instances for each class by minimizing the discrepancy between the marginal distributions of the auxiliary and target domains. This procedure is important because it may occur negative transfer learning due to the dissimilarity between the extra incorporated data and the target

²From multiple domains.

classes for recognition. More specifically, they generalize the Kullback-Leibler Importance Estimation Procedure (KLIEP) for zero-shot learning problem providing a vector with weights \mathbf{w} that are applied to \mathbf{x} jointly with MTL to create an intermediate space.

Fu et al. [19] proposed a transductive multi-view embedding space to alleviate the domain shift problem. To build this latent joint space, they extracted low-level features and projected this representation onto the semantic spaces of multi-view sources (i.e., attributes and word vectors in this case) using single task classifiers (e.g., the same used in [54] or [108]). The vector spaces are combined with Canonical Correlation Analysis (CCA) in order to find linear combinations between the semantic vectors by maximizing the correlation among the attributes. They utilized the eigenvalues of each dimension as a weight estimator that highlights some characteristics for each class. The zero-shot classification is leveraged with a heterogeneous hypergraph-based semi-supervised learning used to explore the manifold structure of the unlabelled data transductively.

Wang and Chen [99] proposed a method based on two stages, i.e., BiDiLEL. In the first stage, a latent embedding space is first created, learning a projection function that maps the visual features onto this low-dimensional subspace. A class landmark is calculated as a mean representation of all instances of that class. In the second stage, an adaptation of Sammon mapping [82] is proposed, called landmark-based Sammon mapping (LSM), responsible for projecting the semantic representation onto the latent space preserving the semantic relatedness between all different classes using the landmarks as guides. The ZSL classification consists of extracting visual features, projecting the representation onto latent space and, searching for the nearest landmark neighbor. Additionally, techniques for post-processing such as self-training and structured prediction were used. Posteriorly, using the BiDiLEL method, Wang and Chen [98] studied different semantic representations for bridging the semantic gap. Their alternative representations are based on textual descriptions of human actions and deep features extracted from still images relevant to human actions. For textual-based descriptions, a corpus obtained from the Wikihow, Wikipedia and Online dictionary is preprocessed with natural language techniques (e.g., obtaining all words in documents and removing stopping words such as “is”, “you”, “of”). The word vectors are represented as average word vectors or Fisher word vectors. On the other hand, for image-based description, a dataset is created using action labels as keywords and relevant images collected with search engines. These images are

inputted into a pre-trained CNN model, where the resultant deep image features are coded as average feature vectors or Fisher feature vectors, resulting in higher performance.

They also investigated the multi-label ZSL problem in [100] based on the observation that, in real scenarios, a video clip conveys multiple human actions corresponding to different concepts and then proposed a multi-label classification method based on a joint ranking embedding learning. However, their main contribution is a novel data split designed specially to this problem. Instead of using a usual instance-first split, they proposed a label-first split in which all the labels are first divided into two mutually exclusive subsets (i.e., seen and unseen). Next, instances that have at least one unseen label are kept for testing, and the rest is taken as seen labels. Hence, the seen subset may be divided into training and validation splits, suitably simulating the real world ZSL scenario.

The method proposed by Gan et al. [24] considers that action classes may share some elements if they are semantically similar to each other. The visual representation is used to learn concept detectors for each class by applying Least Square Regression (LR) as

$$\arg w_k \sum_n (w_k^T x_i - y_i)^2 + \lambda \|w_k\|^2 \quad (4)$$

where $x_i \in \mathbb{R}^d$ is the low-level feature for a video i and $y_i \in \{0, 1\}$ is the associated binary label to the class k . In practice, w is interpreted as the concept detector and λ is a regularization term. The authors explored different values for it (e.g., 0.01, 0.1, 1, 10, 100). They utilized the WordNet hierarchy and the Word2Vec model to infer the semantic similarity between the class labels with a function from Lin [53] and the cosine distance, respectively. Thus, the classification problem can be expressed as

$$p(y_u|x) = \sum_{k=1}^K p(y_u|y_k)p(y_k|x), \quad (5)$$

where $p(y_u|x)$ is the *a posteriori* zero-shot classification probability (for the class y_u given x), $p(y_u|y_k)$ is given by semantic similarity from side information and the concept detectors. The $p(y_k|x)$ is calculated with the concept detectors. Although their promising reported performance, their work only splits the dataset into 90% for seen and 10% for unseen classes, and an evaluation of how the reduced number of seen classes affects the accuracy of the concept detectors is not provided. We believe that performance will be strongly degraded if only 50% of classes were taken as seen.

The main idea of Zhu et al. [116] was to find the most relevant basis to discriminate an action. Then, they combined this information with semantic word embedding to create a generic representation for actions called Universal Representation (UR). UR is computed with Generalised Multiple Instance Learning (GMIL) by evaluating if one instance is more attractive or repulsive to the action class patterns and joining the first ones in bags with pooled Naive Bayes Nearest Neighbor. The UR consists in correlating visual features with semantic information (e.g., word vectors) in a common space $D_s : A \times B$, where $A = E_v(x_s)$ is the visual embedding and $B = E_s$ is the semantic embedding. Non-Negative Matrix Factorization (NMF) is employed to find two non-negative matrices from A and another two to B so that Jansen-Shannon Divergence (JSD) can be applied to preserve the generative components from GMIL, producing the UR. As this approach is focused on cross dataset problem, the domain shift is unknown. The strategy adopted is to use UR to estimate the differences between the classes in the semantic modality. Therefore, using UR, the misalignment observed with semantics are assumed to be reproduced in visual patterns, which is not always true.

Mishra et al. [65] proposed to represent the visual pattern of actions as a Gaussian distribution probability parameters μ_c (mean vector) and σ_c^2 (vector of diagonal covariance). These parameters compound an intermediate subspace θ_c and can be expressed by linear combinations of a set of basis vectors \mathbf{w}_μ or \mathbf{w}_σ guided by semantic attributes (\mathbf{a}_c). For example, $\mu_c = f_\mu(\mathbf{a}_c) = \mathbf{W}_\mu \mathbf{a}_c$. The vector basis $\mathbf{W}_\mu = [\mathbf{w}_{\mu 1}, \mathbf{w}_{\mu 2}, \dots, \mathbf{w}_{\mu K}]$, are learned from attributes or word vectors and the empirical estimates of $\hat{\mu}$ and $\hat{\sigma}^2$ are acquired directly from data with Maximum Likelihood Estimation (MLE) or Maximum-a-Posteriori Estimation (MAP) using linear models (e.g., least square regression) or non-linear model (e.g., kernel regression). These basis vectors can be learned only from seen classes and exploited to unseen action classes. More recently, Mishra et al. [64] investigated the zero-shot learning recognition problem using synthesized features with two distinct approaches: Inverse Autoregressive Flow (IAF) and bi-directional Generative Adversarial Network (GAN). The key idea of the approaches is to generate latent features from attributes or word vectors and then perform zero-shot learning into this embedding space in a supervised manner.

A different strategy for creating a common visual-semantic intermediate space is introduced in [74]. It is based on Error Correcting Output Codes (ECOC) specifically designed for zero shot learning (ZSECOC).

These codes are learned from seen classes by latent factor decomposition and joint optimization³. The codes are represented as \mathbf{B} with $B = \{b_i\}_{i=1}^{|S|} \in \{-1, 1\}^{m \times |S|}$, where m is the dimension of the codes and $|S|$ is the number of seen classes. Aiming to relate seen S and unseen classes \mathcal{U} , the semantic similarity $s_{i,j}$ between each pair of classes in word embedding space is computed with cosine distance in order to transfer these relationships to the codes. This information is stored in a similarity matrix \mathbf{S} . Hence, we have $\mathbf{S}^u = \{s_{i,j}^u\} \in \mathbb{R}^{S \times \mathcal{U}}$ and \mathbf{B}^u is given by $B^u = \text{sign}(\mathbf{B}\mathbf{S}^u)$ where $\text{sign}(\cdot)$ is 1 if the argument is positive and 0 otherwise. The classification is performed by learning binary classifiers based on all the seen data \mathbf{x} and the associated labels. This result in m independent classifiers, one to each bit in the codes $F(\mathbf{x}^u)$. The assignment of a label to unseen instance is done as

$$y^* = \underset{j}{\text{argmin}} d_H(F(\mathbf{x}^u), b_j^u) \quad (6)$$

where d_H denotes the Hamming distance between prior codes and new codes (i.e., predicted with the classifiers).

Many works addressed the relationship between actions and objects or scenes with relative success. For example, Guadarrama et al. [27] proposed an approach based on hierarchical semantic models, where hierarchies are learned to subjects, objects and verbs. Thus, the training step consists of associating visual information with the corresponding leaf in the hierarchy. More specifically, the DTF method is performed to extract handcrafted features and learn a codebook for the entire video. Object detectors from [18] and [51] are used to select the maximum score assigned to each object in any frame. A multi-channel approach combines activities and descriptors of subjects or objects sending this information to a non-linear SVM. Once the leaf classifiers are trained, the nodes are predicted by trading off specificity with semantic similarity, evaluating how semantically close the predicted triplet is to the true action. Therefore, the posterior probabilities of internal nodes are obtained by learning one-vs-all SVM classifiers for the leaf nodes and summing them. With these values, the WUP similarity (from Wu and Palmer [104] work) is computed and the better triplet is predicted.

Jain et al. [34] also described the actions by calculating the detection probability of objects in the video frames utilizing a CNN trained with the ImageNet Dataset. In their method, an entire dataset can be classified without prior knowledge of any action

³We recommend consulting the original paper for mathematical details.

class. Therefore, each video v is represented as $p_v = [p(y_{o_1}, v), \dots, p(y_{o_m}, v)]^T$, where y_{o_m} denotes the m -th object class and $p(y_{o_m}, v)$ is the average of the frame object probabilities⁴ (i.e., the output of the CNN) sampled every 10 frames. The affinity between an object class y_o and an action class y is given by $g_{y_o, y} = s(y_o)^T s(y)$, where $s(\cdot)$ is a semantic embedding of any class (i.e., object class or action class) from Word2Vec. The semantic description of an action class y in function of the object classes is $g_y = [s(y_{o_1}), \dots, s(y_{o_m})]^T s(y)$ and the vector representation of the k most related objects can be estimated by Fisher Vectors. The classification consists of sampling spatio-temporal segments in a video, U_{st} , and applying the following

$$C(v) = \arg \max_{y \in Y, u \in U_{st}} \sum_{y_o} p_{uy_o} g_{y_o, y}. \quad (7)$$

Wu et al. [103] proposed a simple but effective approach to generating an intermediate space that represents the relationships among objects, scenes and actions. In their method, a semantic fusion network fuse three streams: global low-level CNN (e.g., from a VGG19 trained on ImageNet); object features in frames (e.g., from a VGG19 trained on a subset of 20574 objects); and features of scenes (e.g., from a VGG16 trained on Places 205 dataset). These three features are extracted at the frame level, and an average operation computes the scores for the videos. After, the joint features are used to train a three dense layer network composed of two hidden layers and one softmax layer. The correlation between objects/scenes and video classes is mined from the visualization of the network by saliency maps. This procedure produces a matrix with the probability of each pair (object, scene) is related to an action.

Mettes and Snoek [61], on the other hand, proposed a method to classify actions without any video example in the training phase. The method is based on spatial-aware object embeddings, i.e., action tubes scored from interactions between actors and local objects. As prior knowledge, they utilize actions, actors, objects, and their interactions. The similarity between object classes and action classes is provided by the cosine distance from their Word2Vec representations. They proposed a new representation between actor and object exploring where objects tend to occur relative to the actor. This information is acquired using the MS-COCO dataset and the Faster R-CNN for detection of both objects and actors. They also proposed ways to scoring bounding boxes with object interaction and to link spatial-aware

boxes into video tubes (i.e., bounding boxes that localize the actions and their related objects in the space and time). To distinguish tubes from different videos, they utilized global object classifiers through the GoogleLeNet network. The predicted class for a video sample is determined as the class with the highest combined score (i.e., video tube embeddings and global classifiers).

Gao et al. [25] introduced a new strategy to model the semantic relationship between action-attribute⁵, action-action, attribute-attribute. Graph Convolutional Network (GCN) [42] are used in a two-stream configuration. The first stream is responsible for learning classifiers on graph models constructed with ConceptNet5.5 [88] and where the concepts are represented with word vectors in order to have a fixed-length representation. In the second stream, the visual representations of objects (acquired with a combination of the methods used by Jain et al. [34] and Mettes and Snoek [61]) are employed to construct graphs. During training, the classifiers are optimized for the seen categories and are also generalized to zero-shot categories via relationship modeling. At the testing phase, the generated classifiers of unseen categories (i.e., from the first stream) are used to perform the classification on the object features of test videos (i.e., from the second stream).

By observing that ConceptNet has no representations to phrase labels (e.g., playing guitar), Ghosh et al. [26] proposed a novel method to learn knowledge graphs applied to actions. In their method, knowledge graphs are fed to a GCN, and the training objective consists in to minimize the distance between the final classifier layer weights from GCN with the classifier weights layer from I3D. The adopted metric was Mean Squared Error (MSE).

Jones et al. [38] proposed a method to generate semantic embedding spaces based on dynamic attributes signatures. Their method assumes that static attributes are not suitable for modeling actions due to the lack of temporal information. Therefore, finite state machines were constructed over the static annotations provided in the UCF101 and Olympic Sports datasets. For example, they modeled five possible states for each provided attribute: (0): Absence, (1): Persistence, (2): Start, (3): End, and (4): Sometimes. Each state machine contains the transition rules and corresponds to action signatures. The classification is performed by a sequence-level score function over a pre-defined M hypothesized segments. The authors show that this method can also be applied to classification and segmentation tasks.

⁴They utilized 15,293 object categories.

⁵In their work, objects are considered attributes.

Finally, some methods explore multi-modal learning by using video and text pairing. In [112], hierarchical sequential data from videos and text descriptions are modeled. The authors extended the general flat sequence embedding approach that is extensively used (e.g., in video understanding or video captioning). In the original model, paragraphs (i.e., a set of sentences) were represented as a sequence of words that are used in an encoder (e.g., LSTM units or Gated Recurrent Unit (GRU)) to obtain a paragraph embedding. Similarly, videos are a sequence of short clips composed of frames that are used by an encoder to obtain a video embedding.

In this general scheme, the global alignments between the representations are evaluated with a loss function at a high level (e.g., cosine distance). The extension proposed is to add a mid-layer between paragraphs and their embeddings, and between videos and their embeddings. The paragraphs are encoded as a sequence of sentences and the sentences as words (i.e., there are two encoders). In addition to global alignment, local alignments are calculated for mid-layers. The quality of the intermediate encoding is improved by using decoding networks to evaluate reconstruction errors. The ZSL classification occurs through video encoding functions over visual data and textual information alignment.

Piergiovanni and Ryoo [70] also developed a method to learn an intermediate representation for both videos and texts based on an encoder-decoder approach. In their method, there are two pairs of encoder-decoders: (video-encoder) $E_v : v \rightarrow z_v$ and (video-decoder) $G_v : z \rightarrow v$; and (text-encoder) $E_t : t \rightarrow z_t$ and (text-decoder) $G_t : z \rightarrow t$. They used four loss functions (reconstruction, joint, cross-domain, and cycle⁶) to properly treat the learning with paired and unpaired data. The data is paired if we have a pair of video and their descriptive sentence and it is unpaired otherwise. The unpaired learning is conducted in a semi-supervised manner based on adversarial learning by defining three networks (i) to discriminate between text and video-latent representations, (ii) to discriminate the generated video data from the textual information, and (iii) to discriminate the generated textual data from visual information. This last discriminator is especially important when the testing is conducted in datasets such as the UCF101 and HMDB51 that have no captions available because it enables the knowledge transfer. The ActivityNet Captions and Charades Datasets provided the sentences used in the learning process. Once the model is learned, ZSL

classification is conducted by the nearest neighbour rule between each video representation z_v and its text representation z_t in the intermediate space.

3.3. Classification into the visual embedding space

We identify that some recent methods attempt to synthesize the visual features for unseen classes using the features of seen ones and the semantic information. These approaches differ from the two priors because the function learned uses the visual information and the semantic information in the reverse direction. That is, instead of projecting onto semantic space or an intermediate space, the output is given in the visual domain, taking advantage of conditional adversarial learning. For example, Zhang and Peng [113] proposed a multi-level semantic inference method to tackle the problem of modeling the joint distribution of visual features and semantic knowledge and a matching-aware mutual information correlation to solve the semantic gap by transferring semantic knowledge. Briefly, a group of noise is used to synthesize video features, which is simultaneously used by the inference model and the discriminator D to perform semantic inference and correlation constraint. This inference model is responsible for learning an inverse mapping from the synthetic video feature to corresponding semantic knowledge. In the discriminator, two embeddings (i.e., matched and mismatched) are evaluated. After the adversarial training, the model produces visual features classified with the nearest neighbor by evaluating the distance between the generated output and the original visual feature. It is possible to use SVMs and, in this case, the visual features of unseen (i.e., synthesized) and seen categories are merged to train the model in a supervised manner.

Mandal et al. [59] investigated the case of FSL and addressed ZSL as a special case. They proposed to classify if an instance came from the seen or unseen dataset using an out-of-distribution classifier to produce a non-uniform distribution with emphasis on seen categories and a uniformly distributed output on the seen categories. However, to zero-shot learning case, this out-of-distribution classifier is not used and their method became similar to [113], but adapting a Wasserstein GAN [6] conditioned on the embeddings of seen class labels (i.e., in training) and unseen (i.e., in testing). The ZSL classification is made by a classifier that maps the synthesized features to the unseen class labels.

4. Benchmark Datasets

The first popular video benchmarks were small, with approximately 10k videos [12], as shown in Table 4.

⁶We suggest reading the original paper for more details.

Table (4) Datasets used in the ZSAR experiments ordered by year of creation. The number of videos (#V) and the number of classes (#C) are also provided for each dataset.

Datasets	Year	#V	#C	Used in papers
KTH [83]	2004	2391	6	Liu et al. [54]
Weizmann [8]	2005	81	9	Liu et al. [54], Qiu et al. [75]
UCFSports [77]	2008	150	10	Qiu et al. [75], Jain et al. [34]
UIUC [91]	2008	532	14	Liu et al. [54]
Olympic Sports [66]	2010	800	16	Liu et al. [54], Xu et al. [107, 109], Qin et al. [74], Mishra et al. [65], Gao et al. [25], Mandal et al. [59], Mishra et al. [64], Jones et al. [38]
UCF50 [76]	2010	6676	50	Qiu et al. [75]
CCV [37]	2011	9317	20	Xu et al. [108, 109]
HMDB51 [48]	2011	7000	51	Xu et al. [106, 107, 109], Jain et al. [34], Alexiou et al. [5], Wang and Chen [98, 99], Qin et al. [74], Mishra et al. [65], Piergiovanni and Ryoo [70], Zhu et al. [116], Roitberg et al. [80], Hahn et al. [29], Gao et al. [25], Bishay et al. [7], Mandal et al. [59], Mishra et al. [64], Ghosh et al. [26], Brattoli et al. [10]
UCF101 [87]	2012	13320	101	Xu et al. [106], Kodirov et al. [43], Gan et al. [24], Xu et al. [108], Jain et al. [34], Xu et al. [107], Alexiou et al. [5], Xu et al. [109], Wang and Chen [98, 99], Qin et al. [74], Mishra et al. [65], Piergiovanni and Ryoo [70], Zhu et al. [116], Roitberg et al. [80], Hahn et al. [29], Gao et al. [25], Bishay et al. [7], Mandal et al. [59], Mishra et al. [64], Jones et al. [38], Ghosh et al. [26], Brattoli et al. [10]
MPII CC [79, 78]	2012	256	41	Rohrbach et al. [79, 78]
Thumos14 [31]	2014	1574	101	Jain et al. [34]
Breakfast [47]	2014	1989	10	Wang and Chen [100]
ActivityNet [30]	2015	27801	203	Zhang et al. [112], Piergiovanni and Ryoo [70], Wu et al. [103]
Charades [84]	2016	9848	157	Wang and Chen [100], Ghosh et al. [26]
Kinetics 400 [41]	2017	306245	400	Hahn et al. [29]
MLB-YouTube [69]	2018	4290	8	Piergiovanni and Ryoo [70]
Kinetics 700 [11]	2019	650000	700	Brattoli et al. [10]

Larger and complex datasets are available since 2011, such as HMDB51 [48], UCF101 [87], ActivityNet [30] and, more recently, Kinetics [41, 12].

KTH [83] is a dataset with six types of human actions (walking, jogging, running, boxing, hand waving and hand clapping) performed by 25 different people in four different scenarios (outdoors, outdoors with scale variation, outdoors with different clothes, and indoors). The dataset contains 2,391 sequences taken over homogeneous backgrounds with a static camera and a frame rate of 25 frames per second (fps). This dataset is no longer challenging and has not been used to evaluate modern ZSAR methods. Another simple dataset is the Weizmann [8] with nine types of actions (running, walking, jumping-jack, jumping-forward-on-two-legs, jumping-in-place-on-two-legs, galloping-sideways, waving-two-hands, waving-one-hand, and bending) performed by nine different people in low-resolution videos (180×155) with 25 fps.

KTH and Weizmann datasets contain a single staged actor with no occlusion and low clutter. They present video clips with controlled illumination and camera position so that they are not quite representative of the complexity of the real-world scenario and are not used recently. To address these limitations, Kuehne et al. [48] presented the HMDB51 dataset with videos from many sources such as digitized movies, Prelinger archive,

YouTube, and Google videos. This dataset contains 51 actions grouped into 5 categories (general facial actions, facial actions with object manipulation, general body movements, body movements with object interaction, and body movements for human interaction). The height of all the frames is scaled to 240 pixels, and so the width is rescaled, keeping the original aspect ratio. The frame rate is converted to 30 fps in order to ensure consistency in the entire dataset. Due to the complexity of the videos and significant number of videos per class, this dataset is widely used for evaluation.

There are three datasets provided by the University of Central Florida (UCF) that are used in ZSAR: UCF-Sports [77], UCF50 [76] and UCF101 [87]. In these datasets, the complexity grows because the videos are taken from the Web and they contain random camera motion, poor lighting conditions, clutter, as well as changes in scale, appearance and viewpoints, and occasionally no focus on the actions of interest [76]. UCF-Sports, for example, contains 10 actions (diving, golf swing, kicking, lifting, riding horse, running, skateboarding, swing-bench, swing-side and walking) distributed in 150 video sequences with a resolution of 720×480 and 10 fps. This dataset was collected from various sports featured on broadcast television channels, such as BBC and ESPN. On the other hand, UCF50, an extension of the UCF11 dataset [55], contains 50 cat-

egories with a minimum of 100 videos for each action class and a total of 6,676. Finally, UCF101 [87] has 101 action classes with a total of 13,320 videos with frame resolution standardized to 25 fps and resolution to 320×240 pixels and stored in avi format. The action categories are divided into five types (human-object interaction, body-motion only, human-human interaction, playing musical instruments, and sports) and grouped into 25 groups where each group consists of 4-7 videos of an action. This great variation of action types and the largest amount of examples make this dataset widely used in experiments, as well as HMDB51.

Olympic Sports [66] is a complex dataset of activities collected from YouTube sequences. There are 16 activities with 50 sequences per class, and the complex motions go beyond simple punctual or repetitive actions in contrast to UCFSports [77], which contains periodic or simple actions such as walking, running, golf-swing or ball-kicking. Although proposed for activity recognition, this dataset was used in approaches that focus on action recognition [54, 108, 107, 109, 74, 65], demonstrating that the complexity of methods makes them able to work on simple activities. Columbia Consumer Videos (CCV) is a dataset introduced by Jiang et al. [37] and includes 9317 unconstrained videos from the Web, preserving the originality without post-editing. There are 20 semantic categories, including a broader set ranging from events, objects, to scenes annotated using the AMT platform. The number of videos from each category varies from 200 to 800. This dataset is used only in few works [108, 109] because there are examples of actions, activities, objects, and events, being more indicated to video description or retrieval problems. Another limitation is the few number of actions. For example, if a standard protocol that divides in 50% as seen and the rest of unseen classes are performed, the result is a restrict visual space and poor global performance.

MPII Cooking Composites and Breakfast are datasets that contain only cooking activities. MPII Cooking Composites contains 41 basic cooking activities with varying length from 1 to 41 minutes distributed on 256 videos. However, this dataset was used only in the same work where it was introduced. Likewise, Breakfast [47] is a large dataset of daily cooking activities, including a total of 52 participants performing 10 activities in 18 real-life kitchens. The resolution is 320×240 pixels with 15 fps. This dataset was used in a work that explores multi-label zero-shot action recognition [100] because there are 49 action classes annotated⁷ in the clips and

more than one action per clip. Charades dataset [84] is also used in [100] and has activities composed of more than one action. Charades is a challenging dataset built with the collaboration of 267 persons from three continents by using the AMT platform. The objective was to collect videos of common daily activities performed in their homes – especially, examples that are not easy to find on YouTube, movies, or TV broadcasts. The dataset has 9,848 annotated videos representing 157 actions with 30 seconds of duration each. However, as most works do not explore multi-label classification, these datasets are not used for evaluation.

The ActivityNet dataset was introduced by Heilbron et al. [30] and is a large-scale benchmark for human activity understanding. There is a range of complex human activities that are of interest to people in their daily living. More precisely, 203 activity classes with an average of 137 untrimmed videos per class and a total of 27,801 videos. These videos were collected from the Internet, exploring a large amount of video data on online repositories such as YouTube. Around 50% of the videos have a resolution of 1280×720, whereas the majority has 30 fps. This dataset is little explored, possibly due to its high complexity compared to their amount of videos per class (193 on average). It is used in recent works [112, 70, 103], which explore multi-modal learning by combining visual features with textual descriptions. On the Kinetics dataset [41], which is the most extensive collection of human actions available to benchmark, there are 400 complex human action classes from different YouTube videos with at least 400 video clips for each action. The clips are about 10 seconds long, variable resolutions and frame rates. This dataset can be considered the successor of HMDB51, UCF101, and ActivityNet (trimmed version) because it is more suitable for training deep networks from scratch. The HMDB51 and UCF101 datasets are not large enough or have sufficient variation to learn and evaluate the current generation of human action classification models based on deep learning, and this limitation is more evident in zero-shot action recognition. More recently, an extension called Kinetics 700 [11] was used in [10].

As shown in Table 4, there is a group of datasets used only once, such as UIUC [91], Thumos14 [31], and MLB-YouTube [69]. The UIUC dataset is presented in [91]. It consists of 532 high-resolution sequences of 14 activities performed by 8 actors in a single view. The Thumos14 dataset was proposed in the Thumos Challenge context [36]. In this dataset, there are temporally untrimmed videos and background videos, that is, with a similar background but without actions in the scene. The 101 action classes are performed in realis-

⁷ Actions that compound the ten cooking activities.

tic settings and distributed in 1574 video clips. MLB-YouTube [69] is a dataset with activities collected from broadcast baseball videos with a focus on fine-grained activity recognition. More precisely, it is composed of 20 baseball games (42 hours) from the 2017 MLB post-season available on YouTube. In this dataset, the structure of the scene is very similar among activities; often, the only difference is the motion of a single person. Additionally, there is a single camera viewpoint to determine the activity. Due to its objective, this dataset has limited potential in ZSL. A complete description of most of datasets can be found in [13, 39, 86].

5. Experimental Protocols and Performance Analysis

There are many experimental protocols to perform ZSAR in videos. Consequently, it is not easy to compare them. We select works that use HMDB51, UCF101 or Olympic Sports datasets since they are the most popular, as shown in Table 4, which enables comparison among different approaches. The ActivityNet was not selected because we do not discriminate between its two versions (i.e., trimmed and untrimmed) in Table 4. Table 5 reports the results of selected works, the proportions and amount of runs used in experiments and a comparison of performance in inductive and transductive settings. Additionally, we provide complementary information on how the visual and semantic embedding were performed to acquire that result and what was the classification approach.

The approaches are commonly evaluated using a general strategy. Initially, the classes of the dataset are randomly split into two disjoint sets called seen (source) and unseen (target) with different proportions (90%/10%, 80%/20% and 50%/50%). This procedure is repeated many times (3, 5, 10, 30, 50) and, in none work, the chosen proportions and/or the number of runs are justified. We identify three performance metrics reported (i.e., overall accuracy, mean per-class accuracy, and mean average precision). We included the value, rounded to one decimal place, the standard deviation, when was reported, and the measure type.

The motivations for the use of 90%/10%, 80%/20% or 50%/50% splits in each dataset is not clear. It is reasonable to think in terms of the size of the training split. That is, to evaluate whether the method presents better results in the presence of more training information. However, at the same time that they use more information to learn, there are fewer examples to classify and the results tend to be better. On the other hand, in a configuration of 50%/50%, the results tend to be worse

because there are more examples to classify and less information available to learn the models. This behavior is clearly identified in Table 5. In large scale datasets, such as HMDB51 or UCF101, with 50%/50% configuration, it is possible to obtain a relevant amount of videos for both to learn and classify. Thus, this configuration is widely used. Due to the domain shift problem, few works have adopted cross dataset configurations, where the model is trained in one dataset and is evaluated in another. An example is shown in Table 5 marked as 0/20 and 0/50 with impressive results compared with intra-class approaches. Their work performs transfer learning by leveraging object-action relationships.

Large scale datasets are necessary to learn more discriminative models, but the amount of all possible combinations of splits (seen/unseen) for each experiment is enormous. Therefore, it is impractical to perform experiments with all possible combinations and to use random splits is a valid strategy. In this scenario, it is necessary to consider that the experiment is stochastic and that 5 or 10 random splits can be an insufficient sampling compared to all possible combinations. For example, considering the 90/10 split, how statistically significant is a result obtained with 3 or 5 random splits? At the same time, how feasible is to perform the experiments using much more random splits? Thus, we only compare the results of experiments in which the standard deviation was reported. We assume that the mean accuracy has a normal distribution and approximate the population standard deviation σ by sample standard deviation s , and the mean accuracy of population by $\mu \approx \bar{x} \pm E$, where $E \approx t_{95\%,n-1} \frac{s}{\sqrt{n}}$ and $n - 1$ are the degrees of freedom for n runs. When it is impossible to estimate the mean accuracy with 1% of estimation error, it is marked with * and, when it is impossible with 2% it is marked with †.

In 50/50 (seen/unseen) configuration and considering only the inductive setting, the work described by Mandal et al. [59] outperforms all the other methods on HMDB51. On UCF101, the works proposed by Mettes and Snoek [61] and Jones et al. [38] have remarkable results and are based on object-action relationships. On Olympic Sports, the works developed by Mandal et al. [59] and Jones et al. [38] show better performance. Considering the transductive setting, we highlight the results reported by Wang and Chen [99] and Gao et al. [25] on HMDB51, Wang and Chen [99] and Jones et al. [38] on UCF101 and Jones et al. [38] and Gao et al. [25] on Olympic Sports. Next, we point out some considerations on these results.

The BiDiLEL model [99] is based on combina-

Table (5) ZSAR performance on the HMDB51, UCF101 and Olympic Sports datasets. The results are presented rounded to one decimal place for both mean value (\bar{x}) and standard deviation (s), when this value is presented in the original paper. Visual embedding (VE); Semantic embedding (SE); Classification strategy (C); Inductive setting (I); Transductive setting (T); Improved dense trajectories (IDT); Convolutional 3D network (C3D); Inflated 3D network (I3D); Object detector (OD); Attributes (A); Word2Vec (W2V); Global vectors (GloVe); Sentence to vector (S2V); Fisher feature vector (FFV); Classification into the semantic space (SS); Classification into an intermediate space (IS); Classification into the visual space (VS); Overall accuracy (Acc); Mean per-class accuracy (P-c Acc.), and Average precision (AP). * indicates that, in this experiment, is not possible to estimate $\mu = \bar{x} \pm 2.0$ with 95% of confidence. † indicates that, in this experiment, is not possible to estimate $\mu = \bar{x} \pm 2.0$ with 95% of confidence.

%	#	VE	SE	C	Metric	I	HMDB51	I	UCF101	I	Olympic Sports	Reference
							T		T		T	
90/10	3	C3D	W2V	SS	Acc.	51.9	–	49.4	–	–	–	Hahn et al. [29]
	5	IDT	W2V	IS	AP	–	–	81.8	–	–	–	Gan et al. [24]
		I3D	S2V	IS	Acc.	–	–	69.6	–	–	–	Ghosh et al. [26]
80/20	3	C3D	W2V	SS	Acc.	38.2	–	37.4	–	–	–	Hahn et al. [29]
	10	IDT	A+W2V	SS	Acc.	–	–	22.5 ± 3.5†	–	–	–	Kodirov et al. [43]
0/20		OD	W2V	IS	Acc.	–	–	51.2 ± 5.0†	–	–	–	Mettes and Snoek [61]
	30	C3D+IDT	A+W2V	SS	P-c Acc.	–	–	51.1 ± 1.2	66.9 ± 1.9	–	–	Wang and Chen [99]
		C3D	A	SS	Acc.	–	–	42.7 ± 5.4†	–	–	–	Bishay et al. [7]
50/50	3	C3D	W2V	SS	Acc.	24.1	–	22.0	–	–	–	Hahn et al. [29]
	5	IDT	W2V	IS	Acc.	19.7 ± 1.6*	24.8 ± 2.2†	18.3 ± 1.7†	22.9 ± 3.3†	–	–	Xu et al. [107]
	5	IDT	W2V	IS	AP	–	–	–	–	44.3 ± 8.1†	56.6 ± 7.7†	Xu et al. [107]
		C3D	FFV	IS	Acc.	25.8 ± 1.2*	31.5 ± 1.7†	40.1 ± 1.3*	50.6 ± 2.5†	–	–	Wang and Chen [98]
	10	IDT	W2V	SS	Acc.	14.4	22.4	12.0	35.2	–	–	Alexiou et al. [5]
0/50		OD	W2V	IS	Acc.	–	–	40.4 ± 1.0	–	–	–	Mettes and Snoek [61]
		IDT	A+W2V	SS	Acc.	–	–	14.0 ± 1.8*	–	–	–	Kodirov et al. [43]
	30	DTF	W2V	SS	Acc.	18.0 ± 3.0*	21.2 ± 3.0*	12.7 ± 1.6	18.6 ± 2.2	–	–	Xu et al. [106]
		C3D	A	IS	Acc.	–	–	22.7 ± 1.2	24.5 ± 2.9*	50.4 ± 11.2†	57.9 ± 14.1†	Mishra et al. [65]
		C3D	W2V	IS	Acc.	19.3 ± 2.1	20.7 ± 3.1*	17.3 ± 1.1	20.3 ± 1.9	34.1 ± 10.1†	41.3 ± 11.4†	Mishra et al. [65]
		C3D+IDT	A+W2V	SS	P-c Acc.	–	–	26.4 ± 0.6	35.1 ± 1.1	–	–	Wang and Chen [99]
		C3D+IDT	W2V	SS	P-c Acc.	20.6 ± 0.8	22.3 ± 1.1	–	–	–	–	Wang and Chen [99]
		C3D	A	SS	Acc.	–	–	23.2 ± 2.9*	–	–	–	Bishay et al. [7]
		C3D	W2V	SS	Acc.	19.5 ± 4.2*	–	19.0 ± 2.3	–	–	–	Bishay et al. [7]
		I3D	A	VS	P-c Acc.	–	–	38.3 ± 3.0*	–	65.9 ± 8.1†	–	Mandal et al. [59]
		I3D	W2V	VS	P-c Acc.	30.2 ± 2.7*	–	26.9 ± 2.8*	–	50.5 ± 6.9†	–	Mandal et al. [59]
		C3D	A	IS	Acc.	–	–	25.2 ± 3.0*	26.1 ± 3.0*	52.1 ± 11.7†	54.9 ± 11.7†	Mishra et al. [64]
		C3D	W	IS	Acc.	17.5 ± 2.4	21.3 ± 3.2	–	–	–	–	Mishra et al. [64]
		OD	A	IS	P-c Acc.	–	–	48.9 ± 5.8†	48.9 ± 5.8†	74.2 ± 9.9†	74.2 ± 9.9†	Jones et al. [38]
		IDT	A+W	SS	Acc.	–	–	11.7 ± 1.7	22.1 ± 2.5	51.7 ± 11.3†	53.2 ± 11.6†	Xu et al. [109]
		IDT	W	SS	Acc.	14.5 ± 2.7	24.1 ± 3.8*	–	–	–	–	Xu et al. [109]
		IDT	GloVe	VS	Acc.	25.3 ± 4.5*	–	25.4 ± 3.1	–	43.9 ± 7.9†	–	Zhang and Peng [113]
		VGG19	GloVe	VS	Acc.	21.6 ± 5.5*	–	28.8 ± 5.7*	–	35.5 ± 8.9†	–	Zhang and Peng [113]
		OD	W2V	IS	Acc.	23.2 ± 3.0	31.0 ± 3.2	34.2 ± 3.1	41.6 ± 3.7	56.5 ± 6.6*	59.9 ± 5.3*	Gao et al. [25]

tions of features that are projected onto an intermediate space. In the visual extraction step, C3D deep features are combined with IDT handcrafted features and, in the semantic embedding step, a combination of attributes and Word2Vec was used on UCF101, whereas only Word2Vec was used on HMDB51, which was the most powerful combination of features available. This method was applied by Wang and Chen [98] to explore a new semantic embedding method based on static images represented with Fisher vectors.

Table 5 shows that approaches based on simple feature representations extracted with off-the-shelf methods (i.e., Word2Vec, I3D, C3D) were outperformed by methods based on the extraction of more high-level semantic information from video clips, usually with object detection [61, 25] or multi-modal learning (i.e., combining visual information with textual descriptions [112])⁸. This is a remarkable distinction between strategies adapted from object or image ZSL domain and specific strategies for action recognition in videos. Recently, several specific approaches have been proposed, leveraging ZSAR performance.

Zhang and Peng [113] and Mandal et al. [59] utilized GANs to generate more training data from the training set with the same statistic properties and to perform the classification into the visual embedding space. This strategy brings high discriminative power and suffers much less from information degradation than other methods. However, basic GANs suffer from instability in training because they are unrestricted and uncontrollable [101]. Mandal et al. [59] adapted a Wasserstein GAN conditioned on the embeddings of seen and unseen class labels and outperformed the work described by Zhang and Peng [113], which demonstrates the potential of these approaches in the next years. Gao et al. [25] explored the relationship between objects and actions using graph convolutional networks, indicating the effectiveness of using the properties from word vectors to identify relationships between objects-objects and between the objects-actions.

By evaluating the impact of transductive setting on performance, reported in Table 5, it is observed that this configuration presents better results than inductive setting in all works. This is due to the effectiveness of methods as self-training and hubness correction to alleviate the domain shift problem. Although exploring the manifold structure of unseen classes may improve the results, in a real world scenario, this information cannot

be available and inductive approaches are preferable.

Another important consideration is that the use of attributes generally results in better performance than word vectors. For example, using the same method as on UCF101, Mishra et al. [65] obtained 22.7 ± 1.2 with attributes and 17.3 ± 1.1 with Word2Vec. Jones et al. [38] utilized attributes, but modeling their evolution in the clips with finite state machines and acquired promising results. Nevertheless, as discussed previously, the use of attributes is not scalable and become impracticable in real-world scenarios. There is a demand for more strategies to perform semantic embedding, focusing on high-level semantic descriptions based on automatic attribute annotation, objects and scenes relationships with actions or natural language descriptions of videos.

6. Open Issues and Future Work

Although much progress has been made in zero-shot action recognition in the last years, its performance is far from conventional supervised learning. For example, while Carreira and Zisserman [12] obtained 98% and 80.9% of accuracy on UCF101 and HMDB51 datasets using the supervised learning paradigm, respectively, Hahn et al. [29] achieved 21.96% and 24.1% (50%/50% seen/unseen classes), respectively, using the ZSL paradigm and the same I3D model. Even if we compare to the best results in ZSL, that is, those obtained by Mandal et al. [59] ($\sim 38.3 \pm 1.0$) using a generative model, Gao et al. [25] ($\sim 41.6 \pm 1.0$) and Mettes and Snoek [61] ($\sim 40.4 \pm 1.0$) using objects and their relationships with actions, or even Jones et al. [38] using dynamic attributes, we can observe that there is still a lot of room to achieve comparable or useful performance, and this requires to resolve or ameliorate the classical ZSL problem, that is, the semantic gap.

Describing actions is much more challenging than describing nouns. Most works have explored only Word2Vec or GloVe algorithms without modifications or new techniques. As shown in Figure 4, word vectors can present confusions with compound classes (e.g., pommel horse x horse riding). We believe that there are few variations or strategies for semantic embedding. A good example was described by Alexiou et al. [5]. Although the result was not globally superior than other approaches, their work demonstrated that the use of synonyms can leverage the performance of several ZSL methods. Another promising approach to consider compound labels is the sentence to vector model (Sent2Vec) [67], used in [26]. This model was responsible for a speedup of ~ 1.3 compared to the results using Word2Vec in their work. Moreover, we believe that it

⁸Their work has an impressive result but, due to their requirements from textual descriptions, the experiments were conducted on ActivityNet Captions dataset.

is necessary to incorporate more recent advances in language processing, for example, geometric deep learning with Graph Convolutional Networks [111] or explore textual descriptions with transformer-based models, for instance, BERT [15] and VideoBERT [89].

From the perspective of visual extraction, with the recent advances in deep learning methods, its use seems to be imperative, especially pre-trained models, recurrent networks and generative models. However, a new problem emerges. For example, the C3D model is a pre-trained CNN using the Sports-1M Dataset [90]. We believe that using pre-trained deep models in practice means intrinsically to use a cross-dataset approach and, if the same classes that are used to train the deep models were also used to test the ZSL methods, the disjunction between seen and unseen classes would not be respected because the deep model acquires the knowledge from classes that should be unseen. A similar analysis was presented by Roitberg et al. [81], but in the context of cross-dataset studies. They argued that when external datasets are involved, one has to ensure that the terms of ZSL are still met and the seen and unseen categories are disjoint. It is not sufficient to remove only identical classes because there are similar classes, such as Basketball Shooting (UCF101) \times Basketball or Basketball 3 \times 3 or wheelchair basketball (Sports-1M). A protocol to remove semantically similar classes from source category (seen) using the cosine similarity measure and a threshold parameter was defined by Roitberg et al. [81] and this analysis was extended by Brattoli et al. [10]. However, when pre-trained deep models are used, it is necessary to remove the similar classes from the target and not from the source. For example, in [99], we need to compare the classes between UCF101 and Sports-1M (used for training C3D model). It is observed that they share 23 identical classes and 17 similar classes⁹. Since that work uses the same 30 splits employed by Xu et al. [106], these shared classes were not removed from the target before the experiment, so the restriction of ZSL is not preserved. To keep the ZSL disjunction between the training and testing sets, it is necessary to use only unknown classes in the testing time, excluding all classes that were used for training the deep model. In this case, the UCF101 dataset would have 61 possible classes for testing. This approach has been implemented in the work developed by [26]. This new restriction means that it may be impracticable to use the UCF101 or HMDB51 dataset when pre-trained deep models, when C3D or

I3D are used. In fact, as shown in Table 4, more recent datasets, such as Kinetics 600, Kinetics 700 or ARID [110], have not been explored in ZSAR.

We identify that multi-modal learning is a promising approach to address the semantic gap. However, there are few studies with this perspective. Intuitively, it is easier to recognize actions using object detection in the scene or by including more information from still images or texts because the features tend to be more descriptive, as with attributes compared to word embeddings. These alternatives need to be further explored so that we can build robust frameworks for zero-shot action recognition.

As discussed earlier, it is necessary to establish a common protocol and mainly a straight definition of the use of seen classes to fine tuning the parameters of deep models. There is a lack of works in which several experimental protocols are applied to state-of-the-art approaches, so that the community could be able to replicate and compare their results. For example, we believe that an experimental protocol is more suitable for evaluation where there is no need to randomly split the datasets. What criteria could be adopted to define which classes are used in training and which are used in testing? Is it possible to create a general split? If not, what standard should be adopted to create random splits and how many runs would be required?

Answering these questions is critical to the progress of zero-shot learning, but especially in ZSAR because processing videos is more time consuming and requires more hardware infrastructure than processing images. There is no discussion of acceptable classification accuracy, reaction time or resource efficiency in the literature.

We conclude this section by pointing out an interesting and little explored problem that is recognizing whether an example is known or unknown and, based on this information, deciding which approach is more appropriate to try to recognize it. Currently, we find only the works described by Roitberg et al. [80] and Mandal et al. [59] to consider both problems jointly.

7. Conclusions

We presented a survey of available ZSL methods for action recognition in videos that describes several techniques used to perform visual and semantic extraction. We also presented several methods that employ these features and bridge the semantic gap. A comprehensive description of databases and their main applications is provided.

⁹Manual checks.

An analysis of the results was presented along with a discussion of the experimental protocols, from which we can highlight a number of conclusions. First, it is very difficult to compare experimental results since many of them use only one or two specific datasets (for instance, KTH, Weizmann, Charades, Breakfast, MPII Cooking Composites, UCF50) and do not follow the same protocol due to, for instance, differences in split sizes or random runs. To provide a fair comparison, we estimated the mean accuracy of each experiment using the available information and were able to compare experiments that reported standard deviation.

The best results used combinations of features [99], generative models [59], and action-object relationships [25, 71]. Multi-modal approaches (e.g., [112]) also presented promising results, although they are not comparable to most studies due to differences in the experimental protocol.

When comparing the inductive against transductive setting, the results showed that the latter always presented better performance. Although they are not scalable, attributes showed superior results than word vectors, which demonstrates the need to extract high-level semantic information from videos. Finally, it is necessary to further investigate various protocol setups using state-of-the-art methods to identify the best configurations and the criteria for generating the splits, whether fixed or random.

References

References

- [1] Agahian, S., Negin, F., Köse, C., 2020. An efficient human action recognition framework with pose-based spatiotemporal features. *Engineering Science and Technology, an International Journal* 23, 196 – 203.
- [2] Aggarwal, J.K., Ryoo, M.S., 2011. Human activity analysis: A review. *ACM Comput. Surv.* 43, 1–16.
- [3] Akata, Z., Reed, S., Walter, D., Lee, H., Schiele, B., 2015. Evaluation of output embeddings for fine-grained image classification, in: *IEEE Computer Vision and Pattern Recognition (CVPR)*, pp. 2927–2936.
- [4] Al-Naser, M., Ohashi, H., Ahmed, S., Nakamura, K., Akiyama, T., Sato, T., Nguyen, P., Dengel, A., 2018. Hierarchical model for zero-shot activity recognition using wearable sensors, in: *10th International Conference on Agents and Artificial Intelligence*, pp. 478–485.
- [5] Alexiou, I., Xiang, T., Gong, S., 2016. Exploring synonyms as context in zero-shot action recognition, in: *IEEE International Conference on Image Processing*, pp. 4190–4194.
- [6] Arjovsky, M., Chintala, S., Bottou, L., 2017. Wasserstein generative adversarial networks, in: *34th International Conference on Machine Learning, PMLR, International Convention Centre, Sydney, Australia*. pp. 214–223.
- [7] Bishay, M., Zoumpourlis, G., Patras, I., 2019. TARN: Temporal attentive relation network for few-shot and zero-shot action recognition. *CoRR abs/1907.09021*, 1–14.
- [8] Blank, M., Gorelick, L., Shechtman, E., Irani, M., Basri, R., 2005. Actions as space-time shapes, in: *Tenth IEEE International Conference on Computer Vision*, pp. 1395–1402.
- [9] Blei, D.M., Ng, A.Y., Jordan, M.I., 2003. Latent dirichlet allocation. *Journal of Machine Learning Research* 3, 993–1022.
- [10] Brattoli, B., Tighe, J., Zhdanov, F., Perona, P., Chalupka, K., 2020. Rethinking zero-shot video classification: End-to-end training for realistic applications, in: *IEEE Conference on Computer Vision and Pattern Recognition (CVPR)*, pp. 4613–4623.
- [11] Carreira, J., Noland, E., Hillier, C., Zisserman, A., 2019. A short note on the kinetics-700 human action dataset. *CoRR abs/1907.06987*.
- [12] Carreira, J., Zisserman, A., 2017. Quo vadis, action recognition? a new model and the kinetics dataset, in: *2017 IEEE Conference on Computer Vision and Pattern Recognition (CVPR)*, pp. 4724–4733.
- [13] Chaquet, J.M., Carmona, E.J., Fernández-Caballero, A., 2013. A survey of video datasets for human action and activity recognition. *Computer Vision and Image Understanding* 117, 633 – 659.
- [14] Deng, J., Dong, W., Socher, R., Li, L., Li, K., Fei-Fei, L., 2009. Imagenet: A large-scale hierarchical image database, in: *IEEE Conference on Computer Vision and Pattern Recognition*, pp. 248–255.
- [15] Devlin, J., Chang, M., Lee, K., Toutanova, K., 2019. BERT: Pre-training of deep bidirectional transformers for language understanding, in: *Conference of the North American Chapter of the Association for Computational Linguistics: Human Language Technologies, Volume 1 (Long and Short Papers)*, Association for Computational Linguistics, Minneapolis, Minnesota. pp. 4171–4186.
- [16] Dinu, G., Lazaridou, A., Baroni, M., 2014. Improving zero-shot learning by mitigating the hubness problem. *International Conference on Learning Representations*, 1–10.
- [17] Fellbaum, C., 1998. *WordNet: an electronic lexical database*. MIT Press.
- [18] Felzenszwalb, P.F., Girshick, R.B., McAllester, D., Ramanan, D., 2010. Object detection with discriminatively trained part-based models. *IEEE Transactions on Pattern Analysis and Machine Intelligence* 32, 1627–1645.
- [19] Fu, Y., Hospedales, T.M., Xiang, T., Fu, Z., Gong, S., 2014a. Transductive multi-view embedding for zero-shot recognition and annotation, in: *European Conference on Computer Vision*, Springer International Publishing. pp. 584–599.
- [20] Fu, Y., Hospedales, T.M., Xiang, T., Gong, S., 2012. Attribute learning for understanding unstructured social activity, in: *European Conference on Computer Vision*, Springer, Berlin, Heidelberg. pp. 530–543.
- [21] Fu, Y., Hospedales, T.M., Xiang, T., Gong, S., 2014b. Learning multimodal latent attributes. *IEEE Transactions on Pattern Analysis and Machine Intelligence* 36, 303–316.
- [22] Fu, Y., Xiang, T., Jiang, Y., Xue, X., Sigal, L., Gong, S., 2018. Recent advances in zero-shot recognition: Toward data-efficient understanding of visual content. *IEEE Signal Processing Magazine* 35, 112–125.
- [23] Gan, C., Lin, M., Yang, Y., de Melo, G., Hauptmann, A.G., 2016. Concepts not alone: Exploring pairwise relationships for zero-shot video activity recognition, in: *Thirtieth AAAI Conference on Artificial Intelligence*, pp. 3487–3493.
- [24] Gan, C., Lin, M., Yang, Y., Zhuang, Y., Hauptmann, A.G., 2015. Exploring semantic inter-class relationships (SIR) for

- zero-shot action recognition, in: Twenty-Ninth AAAI Conference on Artificial Intelligence, AAAI Press, pp. 3769–3775.
- [25] Gao, J., Zhang, T., Xu, C., 2019. I know the relationships: Zero-shot action recognition via two-stream graph convolutional networks and knowledge graphs, in: Thirty-Third AAAI Conference on Artificial Intelligence, pp. 8303–8311.
- [26] Ghosh, P., Saini, N., Davis, L.S., Shrivastava, A., 2020. All about knowledge graphs for actions. *arXiv preprint arXiv:2008.12432*.
- [27] Guadarrama, S., Krishnamoorthy, N., Malkarnenkar, G., Venugopalan, S., Mooney, R., Darrell, T., Saenko, K., 2013. YouTube2Text: Recognizing and describing arbitrary activities using semantic hierarchies and zero-shot recognition, in: IEEE International Conference on Computer Vision, pp. 2712–2719.
- [28] Guo, G., Lai, A., 2014. A survey on still image based human action recognition. *Pattern Recognition* 47, 3343–3361.
- [29] Hahn, M., Silva, A., Reh, J.M., 2019. Action2Vec: A cross-modal embedding approach to action learning, in: IEEE Conference on Computer Vision and Pattern Recognition, (CVPR) Workshops, pp. 1–10.
- [30] Heilbron, F.C., Escorcia, V., Ghanem, B., Niebles, J.C., 2015. ActivityNet: A large-scale video benchmark for human activity understanding, in: IEEE Conference on Computer Vision and Pattern Recognition (CVPR), pp. 961–970.
- [31] Idrees, H., Zamir, A.R., Jiang, Y., Ghorban, A., Laptev, I., Sukthankar, R., Shah, M., 2017. The THUMOS challenge on action recognition for videos “in the wild”. *Computer Vision and Image Understanding* 155, 1–23.
- [32] Ikizler-Cinbis, N., Sclaroff, S., 2010. Object, scene and actions: Combining multiple features for human action recognition, in: European Conference on Computer Vision (ECCV), Springer Berlin Heidelberg, Berlin, Heidelberg, pp. 494–507.
- [33] Ioffe, S., Szegedy, C., 2015. Batch normalization: Accelerating deep network training by reducing internal covariate shift, in: 32nd International Conference on Machine Learning, JMLR, pp. 448–456.
- [34] Jain, M., van Gemert, J.C., Mensink, T., Snoek, C.G.M., 2015. Objects2Action: Classifying and localizing actions without any video example, in: IEEE International Conference on Computer Vision (ICCV), pp. 4588–4596.
- [35] Ji, S., Xu, W., Yang, M., Yu, K., 2013. 3D convolutional neural networks for human action recognition. *IEEE Transactions on Pattern Analysis and Machine Intelligence* 35, 221–231.
- [36] Jiang, Y., Liu, J., Zamir, A.R., Toderici, G., Laptev, I., Shah, M., Sukthankar, R., 2014. THUMOS challenge: Action recognition with a large number of classes. <http://csrc.ucf.edu/THUMOS14/>.
- [37] Jiang, Y., Ye, G., Chang, S., Ellis, D., Loui, A.C., 2011. Consumer video understanding: a benchmark database and an evaluation of human and machine performance, in: Annual ACM International Conference on Multimedia Retrieval, pp. 1–8.
- [38] Jones, J.D., Kim, T.S., Peven, M., Xiao, Z., Bai, J., Zhang, Y., Qiu, W., Yuille, A., Hager, G.D., 2019. DAZSL: Dynamic attributes for zero-shot learning. *arXiv*, 1–18.
- [39] Kang, S., Wildes, R.P., 2016. Review of action recognition and detection methods. *CoRR abs/1610.06906*.
- [40] Karpathy, A., Toderici, G., Shetty, S., Leung, T., Sukthankar, R., Fei-Fei, L., 2014. Large-scale video classification with convolutional neural networks, in: IEEE Conference on Computer Vision and Pattern Recognition (CVPR), pp. 1725–1732.
- [41] Kay, W., Carreira, J., Simonyan, K., Zhang, B., Hillier, C., Vijayanarasimhan, S., Viola, F., Green, T., Back, T., Natsev, A., Suleyman, M., Zisserman, A., 2017. The kinetics human action video dataset. *CoRR abs/1705.06950*, 1–22.
- [42] Kipf, T., Welling, M., 2017. Semi-supervised classification with graph convolutional networks, in: 5th International Conference on Learning Representations (ICRL), pp. 1–14.
- [43] Kodirov, E., Xiang, T., Fu, Z., Gong, S., 2015. Unsupervised domain adaptation for zero-shot learning, in: IEEE International Conference on Computer Vision (CVPR), pp. 2452–2460.
- [44] Kong, Y., Fu, Y., 2018. Human action recognition and prediction: A survey. *ArXiv abs/1806.11230*.
- [45] Köpüklü, O., Gunduz, A., Kose, N., Rigoll, G., 2019. Real-time hand gesture detection and classification using convolutional neural networks. *CoRR*.
- [46] Krizhevsky, A., Sutskever, I., Hinton, G.E., 2012. ImageNet classification with deep convolutional neural networks, in: 25th International Conference on Neural Information Processing Systems, Curran Associates Inc., USA, pp. 1097–1105.
- [47] Kuehne, H., Arslan, A.B., Serre, T., 2014. The language of actions: Recovering the syntax and semantics of goal-directed human activities. *IEEE Conference on Computer Vision and Pattern Recognition (CVPR)*, 780–787.
- [48] Kuehne, H., Jhuang, H., Garrote, E., Poggio, T., Serre, T., 2011. HMDB: A large video database for human motion recognition, in: International Conference on Computer Vision (ICCV), pp. 2556–2563.
- [49] Lampert, C.H., Nickisch, H., Harmeling, S., 2009. Learning to detect unseen object classes by between-class attribute transfer, in: IEEE Conference on Computer Vision and Pattern Recognition, pp. 951–958.
- [50] Laroca, R., Severo, E., Zanlorensi, L.A., Oliveira, L.S., Gonçalves, G.R., Schwartz, W.R., Menotti, D., 2018. A robust real-time automatic license plate recognition based on the YOLO detector, in: 2018 International Joint Conference on Neural Networks (IJCNN), pp. 1–10.
- [51] Li, L., Su, H., Fei-Fei, L., Xing, E.P., 2010. Object Bank: A high-level image representation for scene classification & semantic feature sparsification, in: Lafferty, J.D., Williams, C.K.I., Shawe-Taylor, J., Zemel, R.S., Culotta, A. (Eds.), *Advances in Neural Information Processing Systems 23*. Curran Associates, Inc., pp. 1378–1386.
- [52] Li, Y., Hu, S., Li, B., 2016. Recognizing unseen actions in a domain-adapted embedding space, in: IEEE International Conference on Image Processing (ICIP), pp. 4195–4199.
- [53] Lin, D., 1998. An information-theoretic definition of similarity, in: Fifteenth International Conference on Machine Learning, Morgan Kaufmann Publishers Inc., San Francisco, CA, USA, p. 296–304.
- [54] Liu, J., Kuipers, B., Savarese, S., 2011. Recognizing human actions by attributes, in: IEEE Conference on Computer Vision and Pattern Recognition (CVPR), IEEE Computer Society, Washington, DC, USA, pp. 3337–3344.
- [55] Liu, J., Luo, J., Shah, M., 2009. Recognizing realistic actions from videos “in the wild”, in: IEEE Conference on Computer Vision and Pattern Recognition (CVPR), pp. 1996–2003.
- [56] Liu, K., Liu, W., Ma, H., Huang, W., Dong, X., 2018a. Generalized zero-shot learning for action recognition with web-scale video data. *World Wide Web* 22, 807–824.
- [57] Liu, L., Wang, S., Hu, B., Qiong, Q., Wen, J., Rosenblum, D.S., 2018b. Learning structures of interval-based bayesian networks in probabilistic generative model for human complex activity recognition. *Pattern Recognition* 81, 545 – 561.
- [58] van der Maaten, L., Hinton, G., 2008. Visualizing data using t-sne. *Journal of Machine Learning Research* 9, 2579–2605.
- [59] Mandal, D., Narayan, S., Dwivedi, S.K., Gupta, V., Ahmed, S., Khan, F.S., Shao, L., 2019. Out-of-distribution detection for generalized zero-shot action recognition, in: IEEE Conference on Computer Vision and Pattern Recognition (CVPR), pp.

- 9985–9993.
- [60] Menotti, D., Chiachia, G., da Silva Pinto, A., Schwartz, W.R., Pedrini, H., Falcão, A.X., Rocha, A., 2015. Deep representations for iris, face, and fingerprint spoofing detection. *IEEE Trans. Inf. Forensics Secur.* 10, 864–879.
 - [61] Mettes, P., Snoek, C.G.M., 2017. Spatial-aware object embeddings for zero-shot localization and classification of actions, in: *IEEE International Conference on Computer Vision*, pp. 1–10.
 - [62] Mikolov, T., Sutskever, I., Chen, K., Corrado, G., Dean, J., 2013a. Distributed representations of words and phrases and their compositionality, in: *26th International Conference on Neural Information Processing Systems (NIPS)*, Curran Associates Inc., USA. pp. 3111–3119.
 - [63] Mikolov, T., Yih, W., Zweig, G., 2013b. Linguistic regularities in continuous space word representations, in: *Conference of the North American Chapter of the Association for Computational Linguistics: Human Language Technologies*, Association for Computational Linguistics. pp. 746–751.
 - [64] Mishra, A., Pandey, A., Murthy, H.A., 2020. Zero-shot learning for action recognition using synthesized features. *Neurocomputing* 390, 117–130.
 - [65] Mishra, A., Verma, V.K., Reddy, M.S.K., Subramaniam, A., Rai, P., Mittal, A., 2018. A generative approach to zero-shot and few-shot action recognition, in: *IEEE Winter Conference on Applications of Computer Vision (WACV)*, pp. 372–380.
 - [66] Niebles, J.C., Chen, C., Fei-Fei, L., 2010. Modeling temporal structure of decomposable motion segments for activity classification, in: *European Conference on Computer Vision (ECCV)*, Springer Berlin Heidelberg, Berlin, Heidelberg. pp. 392–405.
 - [67] Pagliardini, M., Gupta, P., Jaggi, M., 2018. Unsupervised learning of sentence embeddings using compositional n-gram features, in: *Proceedings of the 2018 Conference of the North American Chapter of the Association for Computational Linguistics: Human Language Technologies, Volume 1 (Long Papers)*, Association for Computational Linguistics, New Orleans, Louisiana. pp. 528–540.
 - [68] Pennington, J., Socher, R., Manning, C.D., 2014. GloVe: Global vectors for word representation, in: *Conference on Empirical Methods in Natural Language Processing (EMNLP)*, pp. 1532–1543.
 - [69] Piergiovanni, A., Ryoo, M.S., 2018a. Fine-grained activity recognition in baseball videos, in: *IEEE Conference on Computer Vision and Pattern Recognition Workshops (CVPRW)*, pp. 1853–1861.
 - [70] Piergiovanni, A., Ryoo, M.S., 2018b. Learning shared multimodal embeddings with unpaired data. *CoRR* abs/1806.08251.
 - [71] Poppe, R., 2010. A survey on vision-based human action recognition. *Image and Vision Computing* 28, 976–990.
 - [72] Pouyanfar, S., Sadiq, S., Yan, Y., Tian, H., Tao, Y., Reyes, M.P., Shyu, M.L., Chen, S.C., Iyengar, S.S., 2018. A survey on deep learning: Algorithms, techniques, and applications. *ACM Computing Surveys* 51, 92:1–36.
 - [73] Prest, A., Schmid, C., Ferrari, V., 2012. Weakly supervised learning of interactions between humans and objects. *IEEE Transactions on Pattern Analysis and Machine Intelligence* 34, 601–614.
 - [74] Qin, J., Liu, L., Shao, L., Shen, F., Ni, B., Chen, J., Wang, Y., 2017. Zero-shot action recognition with error-correcting output codes, in: *IEEE Conference on Computer Vision and Pattern Recognition (CVPR)*, pp. 1042–1051.
 - [75] Qiu, Q., Jiang, Z., Chellappa, R., 2011. Sparse dictionary-based representation and recognition of action attributes, in: *IEEE International Conference on Computer Vision (ICCV)*, pp. 707–714.
 - [76] Reddy, K.K., Shah, M., 2013. Recognizing 50 human action categories of web videos. *Machine Vision and Applications* 24, 971–981.
 - [77] Rodriguez, M.D., Ahmed, J., Shah, M., 2008. Action MACH a spatio-temporal maximum average correlation height filter for action recognition, in: *IEEE Conference on Computer Vision and Pattern Recognition (CVPR)*, pp. 1–8.
 - [78] Rohrbach, M., Ebert, S., Schiele, B., 2013. Transfer learning in a transductive setting, in: *26th International Conference on Neural Information Processing Systems*, Curran Associates, Inc., pp. 46–54.
 - [79] Rohrbach, M., Regneri, M., Andriluka, M., Amin, S., Pinkal, M., Schiele, B., 2012. Script data for attribute-based recognition of composite activities, in: *European Conference on Computer Vision (ECCV)*, Springer Berlin Heidelberg, Berlin, Heidelberg. pp. 144–157.
 - [80] Roitberg, A., Al-Halah, Z., Stiefelhausen, R., 2018a. Informed democracy: Voting-based novelty detection for action recognition, in: *British Machine Vision Conference (BMVC)*, pp. 1–14.
 - [81] Roitberg, A., Martinez, M., Haurilet, M., Stiefelhausen, R., 2018b. Towards a fair evaluation of zero-shot action recognition using external data, in: *European Conference on Computer Vision (ECCV) Workshops*, pp. 1–9.
 - [82] Sammon, J.W., 1969. A nonlinear mapping for data structure analysis. *IEEE Transactions on Computers* C-18, 401–409.
 - [83] Schödl, C., Laptev, I., Caputo, B., 2004. Recognizing human actions: A local svm approach, in: *International Conference on Pattern Recognition (ICPR)*, pp. 32–36.
 - [84] Sigurdsson, G.A., Varol, G., Wang, X., Farhadi, A., Laptev, I., Gupta, A., 2016. Hollywood in homes: Crowdsourcing data collection for activity understanding, in: *European Conference on Computer Vision (ECCV)*, Springer International Publishing. pp. 510–526.
 - [85] Simonyan, K., Zisserman, A., 2015. Very deep convolutional networks for large-scale image recognition, in: *3rd International Conference on Learning Representations, ICLR*, pp. 1–14.
 - [86] Singh, R., Sonawane, A., Srivastava, R., 2019. Recent evolution of modern datasets for human activity recognition: a deep survey. *Multimedia Systems* 24, 1–24.
 - [87] Soomro, K., Zamir, A.R., Shah, M., 2012. UCF101: A dataset of 101 human actions classes from videos in the wild. *CoRR*, 1–6.
 - [88] Speer, R., Chin, J., Havasi, C., 2017. ConceptNet 5.5: An open multilingual graph of general knowledge, in: *Thirty-First AAAI Conference on Artificial Intelligence*, AAAI Press. pp. 4444–4451.
 - [89] Sun, C., Myers, A., Vondrick, C., Murphy, K., Schmid, C., 2019. VideoBERT: A joint model for video and language representation learning, in: *IEEE International Conference on Computer Vision (ICCV)*, pp. 7463–7472.
 - [90] Tran, D., Bourdev, L., Fergus, R., Torresani, L., Paluri, M., 2015. Learning spatiotemporal features with 3d convolutional networks, in: *IEEE International Conference on Computer Vision (ICCV)*, IEEE Computer Society, Washington, DC, USA. pp. 4489–4497.
 - [91] Tran, D., Sorokin, A., 2008. Human activity recognition with metric learning, in: *European Conference on Computer Vision (ECCV)*, Springer Berlin Heidelberg, Berlin, Heidelberg. pp. 548–561.
 - [92] Tran, D., Wang, H., Torresani, L., Ray, J., LeCun, Y., Paluri, M., 2018. A closer look at spatiotemporal convolutions for action recognition, in: *IEEE Conference on Computer Vision and Pattern Recognition (CVPR)*, pp. 6450–6459.

- [93] Turaga, P., Chellappa, R., Subrahmanian, V.S., Udrea, O., 2008. Machine recognition of human activities: A survey. *IEEE Transactions on Circuits and Systems for Video Technology* 18, 1473–1488.
- [94] Wang, H., Kläser, A., Schmid, C., Liu, C., 2011. Action recognition by dense trajectories, in: *IEEE Conference on Computer Vision and Pattern Recognition (CVPR)*, pp. 3169–3176.
- [95] Wang, H., Kläser, A., Schmid, C., Liu, C., 2013. Dense trajectories and motion boundary descriptors for action recognition. *International Journal of Computer Vision* 103, 60–79.
- [96] Wang, H., Oneata, D., Verbeek, J., Schmid, C., 2016. A robust and efficient video representation for action recognition. *Int. J. Comput. Vision* 119, 219–238.
- [97] Wang, H., Schmid, C., 2013. Action recognition with improved trajectories, in: *IEEE International Conference on Computer Vision (ICCV)*, pp. 3551–3558.
- [98] Wang, Q., Chen, K., 2017a. Alternative semantic representations for zero-shot human action recognition, in: *Machine Learning and Knowledge Discovery in Databases - European Conference, ECML PKDD 2017, Skopje, Macedonia, September 18–22, 2017, Proceedings, Part I*, pp. 87–102.
- [99] Wang, Q., Chen, K., 2017b. Zero-shot visual recognition via bidirectional latent embedding. *International Journal of Computer Vision* 124, 356–383.
- [100] Wang, Q., Chen, K., 2020. Multi-label zero-shot human action recognition via joint latent ranking embedding. *Neural Networks* 122, 1–23.
- [101] Wang, S., Gao, H., Zhu, Y., Zhang, W., Chen, Y., 2019a. A food dish image generation framework based on progressive growing GANs, in: *Collaborative Computing: Networking, Applications and Worksharing*, Springer International Publishing, Cham. pp. 323–333.
- [102] Wang, W., Zheng, V.W., Yu, H., Miao, C., 2019b. A survey of zero-shot learning: Settings, methods, and applications. *ACM Transactions on Intelligent Systems and Technology* 10, 1–37.
- [103] Wu, Z., Fu, Y., Jiang, Y., Sigal, L., 2016. Harnessing object and scene semantics for large-scale video understanding, in: *IEEE Conference on Computer Vision and Pattern Recognition (CVPR)*, IEEE Computer Society. pp. 3112–3121.
- [104] Wu, Z., Palmer, M., 1994. Verbs semantics and lexical selection, in: *32nd Annual Meeting on Association for Computational Linguistics*, Association for Computational Linguistics, USA. pp. 133–138.
- [105] Xian, Y., Schiele, B., Akata, Z., 2017. Zero-shot learning - the good, the bad and the ugly, in: *IEEE Conference on Computer Vision and Pattern Recognition (CVPR)*, pp. 3077–3086.
- [106] Xu, X., Hospedales, T., Gong, S., 2015. Semantic embedding space for zero-shot action recognition, in: *IEEE International Conference on Image Processing (ICIP)*, pp. 63–67.
- [107] Xu, X., Hospedales, T., Gong, S., 2016. Multi-task zero-shot action recognition with prioritised data augmentation, in: *European Conference on Computer Vision (ECCV)*, pp. 343–359.
- [108] Xu, X., Hospedales, T., Gong, S., 2017a. Transductive zero-shot action recognition by word-vector embedding. *International Journal of Computer Vision* 123, 309–333.
- [109] Xu, X., Hospedales, T., Gong, S., 2017b. Transductive zero-shot action recognition by word-vector embedding. *International Journal of Computer Vision* 123, 309–333.
- [110] Xu, Y., Yang, J., Cao, H., Mao, K., Yin, J., See, S., 2020. ARID: A new dataset for recognizing action in the dark. *CoRR*, 1–8.
- [111] Yao, T., Li, Y., Qiu, Z., Long, F., Pan, Y., Li, D., Mei, T., 2017. Trimmed action recognition, temporal action proposals and dense-captioning events in videos, in: *Proceedings of the MSR Asia MSM at ActivityNet Challenge 2017*, pp. 1–6.
- [112] Zhang, B., Hu, H., Sha, F., 2018. Cross-modal and hierarchical modeling of video and text, in: *European Conference on Computer Vision (ECCV)*, Springer International Publishing. pp. 385–401.
- [113] Zhang, C., Peng, Y., 2018. Visual data synthesis via GAN for zero-shot video classification, in: *Twenty-Seventh International Joint Conference on Artificial Intelligence (IJCAI)*, AAAI Press. pp. 1128–1134.
- [114] Zhang, Y., Qu, W., Wang, D., 2014. Action-scene model for human action recognition from videos. *AASRI Procedia* 6, 111 – 117. 2nd AASRI Conference on Computational Intelligence and Bioinformatics.
- [115] Zhang, Z., Wang, C., Xiao, B., Zhou, W., Liu, S., 2013. Attribute regularization based human action recognition. *IEEE Transactions on Information Forensics and Security* 8, 1600–1609.
- [116] Zhu, Y., Long, Y., Guan, Y., Newsam, S.D., Shao, L., 2018. Towards universal representation for unseen action recognition, in: *IEEE Conference on Computer Vision and Pattern Recognition (CVPR)*, pp. 9436–9445.
- [117] Ziaefard, M., Bergevin, R., 2015. Semantic human activity recognition: A literature review. *Pattern Recognition* 48, 2329–2345.